

High-order harmonic generation with resonant core excitation by ultraintense x rays*

Christian Buth[†]

*Max-Planck-Institut für Kernphysik, Saupfercheckweg 1, 69117 Heidelberg, Germany and
Theoretische Chemie, Physikalisch-Chemisches Institut, Ruprecht-Karls-Universität Heidelberg,
Im Neuenheimer Feld 229, 69120 Heidelberg, Germany*

(Dated: 15 Oct 2015)

High-order harmonic generation (HHG) is combined with resonant x-ray excitation of a core electron into the transient valence vacancy that is created in the course of the HHG process. To describe this setting, I develop a two-active-electron quantum theory for a single atom assuming no Coulomb interaction among the electrons; one electron performs a typical HHG three-step process whereas another electron is excited (or even Rabi flops) by intense x rays from the core shell into the valence hole after the first electron has left the atom. Depending on the amplitude to find a vacancy in the valence and the core, the returning continuum electron recombines with the valence and the core, respectively, emitting high-order harmonic (HH) radiation that is characteristic of the combined process. After presenting the theory of x-ray boosted HHG for continuous-wave light fields, I develop a description for x-ray pulses with a time-varying amplitude and phase. My prediction offers novel prospects for nonlinear x-ray physics, attosecond x rays, and HHG-based time-dependent chemical imaging involving core orbitals.

PACS numbers: 42.65.Ky: Frequency conversion; harmonic generation, including higher-order harmonic generation — 32.80.Aa: Inner-shell excitation and ionization — 32.30.Rj: X-ray spectra — 41.60.Cr: Free-electron lasers

Keywords: x rays – optical laser – photoionization – core-hole decay – high-order harmonic generation – HHG – x-ray free electron laser – FEL – Rabi flopping – strong-field physics

I. INTRODUCTION

Since the discovery of high-order harmonic generation (HHG) by atoms in intense optical laser fields [1, 2], HHG has spawned the field of attoscience, is used for spectroscopy, and serves as a light source in many optical laboratories [3–7]. Initially, there has been a period of learning about the fundamental physics of HHG [8, 9] which lead to a phenomenological description by a single atom in terms of a three-step model [10, 11] and quantum theories [12–17]. Soon it was realized that high-order harmonic (HH) light from a dense gas is not well-described by the HH spectrum of a single atom and one needs to account for propagation effects of the optical laser and the HH radiation in the macroscopic medium [18–22]. Nowadays, more and more applications based on HHG have come into focus [see, e.g., Refs. 3–7]. To name a few, in atoms, there is the phase measurement of resonant two-photon ionization in helium [23] and intense x-ray generation [22]; for molecules, there is tomographic imaging of orbitals and related methods for structure determination [24–29], and the control of electron localization in photodissociation [30]. Finally, for condensed matter, an attosecond spectroscopy has been developed [31].

Present-day canonical theory of HHG [3–7] gravitates around HHG from valence electrons and the single-active electron (SAE) approximation [32, 33]. Within the SAE

approximation and the three-step model of HHG [10, 11], the optical laser tunnel ionizes a valence electron and accelerates it in the continuum. When the optical laser field changes direction, the liberated electron is driven back to rescatter with the parent ion. This may cause the electron to recombine with the ion whereby the excess energy due to the atomic potential and due to the energy gained from the optical laser field is released in terms of a photon with an energy which is a high-order harmonic of the optical frequency. In HHG each rescattering generates attosecond bursts of radiation [34]. HHG from an ultrashort optical laser pulse leads to an attosecond pulse train [35] in which the individual attosecond pulses are separated by a half cycle period of the optical laser from which a single attosecond burst can be isolated by filtering out the harmonics close to the HH cutoff (maximum photon energy for a given optical laser intensity) [36]. By optimizing the quantum path of the continuum electron, the HH cutoff can be increased by a factor of 2.5 [37].

Explorations beyond the canonical theory of HHG [3–7] have been pursued in only a few works. In Refs. 38–41, HHG from a coherent superposition of the ground state and an excited state of an atom was investigated. A shift of the HH spectrum was found amounting to the energy difference between the two states involved with the unshifted and the shifted plateaux having a similar height. In Ref. 42 HHG for a parent ion that is described by a potential that has an autoionizing state is reported for HHG from laser-ablation of solids; a four-level model is proposed in which the recombination from an electron trapped in the autoionizing state to the ground state occurs. The autoionizing state is populated by a radiationless transition of the returning continuum electron.

* The final publication is available at Springer via [dx.doi.org/10.1140/epjd/e2015-60357-3](https://doi.org/10.1140/epjd/e2015-60357-3).

[†] World Wide Web: www.christianbuth.name, electronic mail; christian.buth@web.de

A one- to two-order of magnitude enhancement of HH intensity for a harmonic that is resonant with the transition between the autoionizing state and the ground state is observed. A somewhat different modeling based on a modification of the model of Lewenstein *et al.* [12] with a coherent superposition of states with a thorough numerical investigation of the intensity and phase of resonant high harmonics is presented in Ref. 43. Recently, it was both experimentally observed and theoretically explained in Refs. 44 and 45 that molecular orbitals below the highest occupied molecular orbital have a significant impact on HH emission; the authors of Ref. 46 investigate in strong-field approximation [12] the influence of quantum interference on HH spectra of molecules with two optically active electrons from different orbitals. In Ref. 47 a coherent superposition of states in dynamically aligned molecules was exploited to measure the time-evolution of the molecular dynamics with high sensitivity. Multiple cutoffs from plasmon-like excitations in ions were predicted in Ref. 48. The role of multielectron effects regarding the recombination probability of the recolliding electron was discussed in Refs. 28 and 49. Further a two-electron scheme was considered that uses sequential double ionization by an optical laser with a subsequent nonsequential double recombination; in helium it leads to a second plateau with about 12 orders of magnitude lower yield than the primary HH plateau [50].

Frequently, the SAE approximation for a valence electron is also applied to two-color HHG where an optical laser is combined with VUV/XUV light; the high-frequency radiation assists, thereby, in the ionization process leading to an overall increased yield [51–54]. Two-color HHG is evolved further by using attosecond XUV pulses to manipulate the HHG process which increases the HH yield for a certain frequency range by enhancing the contribution from specific quantum orbits [55–60]. However, there are only few exceptions, e.g., Refs. 28, 49, 61, and 62, in which many-electron effects are treated for two-color HHG. In Refs. 61 and 62 the influence of other electrons is included implicitly by using a frequency-dependent polarizability for the atoms: the XUV light is found to cause new plateaux to emerge at higher energies, however, with a much lower HH yield.

Alternatively to HHG-based light sources for XUV light and, particularly, x rays, there are synchrotrons and—most relevant for this work—the newly constructed free electron lasers (FELs) that provide exciting opportunities for strong-field physics. For example, the Free Electron Laser in Hamburg (FLASH) [63] offers XUV to soft x-ray radiation that is ideal for studying the valence and shallow core of atoms or the Linac Coherent Light Source (LCLS) [64, 65] which delivers soft and hard x rays suitable for x-ray diffraction with atomic resolution and examining core electrons of the elements in the periodic table. Existing high-frequency FELs produce XUV- and x-ray light of unprecedented intensity which can be used—among many other applications—to manipulate optical strong-field processes. They operate according

to the self-amplification of spontaneous emission (SASE) principle which produces chaotic light [66–68] that can be modeled by the partial coherence method (PCM) [69–71].

The combination of an optical laser and XUV/x-ray light from synchrotrons or FELs has proven to be very beneficial in the past, e.g., to control the interaction of the x rays with optical light in various ways involving atoms and molecules [72–75]. Recently, x-ray and optical wave mixing—specifically sum-frequency generation (SFG) of optical light and x rays—was demonstrated at LCLS by Glover *et al.* [76] with a conversion efficiency of 3×10^{-7} . Such x-ray and optical wave mixing was proposed theoretically [77–79] many years ago in the 1970s but only recently it has become feasible to observe SFG experimentally by the construction of FELs with unprecedented x-ray intensity [76]. The experiment of Glover *et al.* is an encouraging motivation of theoretical research on x-ray boosted HHG in which HHG is modified by x rays [80–82] because SFG is the simplest way to boost x rays by optical light. Within the SAE, HHG with core electrons of neon that are ionized by x rays were studied theoretically [82]. A single-atom efficiency comparable with conventional HHG was found and attosecond pulses were isolated from the x-ray-boosted HH spectra. The theory of Ref. [82] is a form of laser-assisted x-ray-atom scattering extensively examined for hydrogen atoms in Refs. 83 and 84 and Refs. therein generalized to multielectron atoms.

Since the publication of the articles [80–82] and a preprint of this work [85] a few related or inspired articles have been published. Using the resonant interaction of XUV light with an atomic transition in hydrogen-like atoms that are strongly perturbed by optical light Antonov *et al.* [86] predict attosecond pulse generation based on resonant interaction in a macroscopic medium for VUV or XUV light. My prediction of a splitting of HH peaks by Rabi oscillations is demonstrated in Ref. 87 where an optical laser and intense XUV light is used jointly to predict HHG from a model potential where two cases are explored: first, a system with two bound states; second, a system with a shape resonance

In this work, I devise a detailed theory of HHG by an optical laser with resonant excitation (or even Rabi flopping [88–93]) of a core electron in intense XUV/x-ray light. Specifically, I will focus on the case of continuous-wave (cw) light, first, constant-amplitude light with finite pulse duration, second, and a constant-amplitude optical laser in combination with arbitrary x-ray pulses, third. In the parlance of the three-step model [10, 11], x-ray-boosted HHG [Fig. 1] proceeds as follows: first, the atomic valence is tunnel ionized; second, the liberated electron propagates freely in the electric field of the optical laser; third, the direction of the optical laser field is reversed and the continuum electron is driven back to the parent ion and rescatters with it which may cause it to recombine with the vacancy emitting the excess energy in terms of a HH photon. The excursion time of

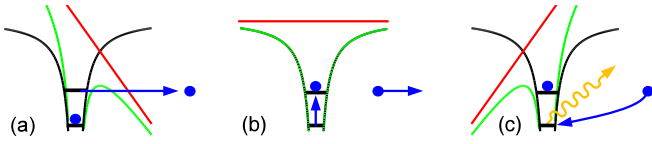


FIG. 1. (Color online) Schematic of the three-step model of HHG [10, 11] augmented by resonant x-ray excitation of core electrons: (a) tunnel ionization of a valence electron in the optical laser field; (b) while the first electron propagates freely in the continuum, a second electron from a core orbital is excited into the transient valence hole; (c) eventually, the continuum electron is driven back to the residual ion by a reversal of the direction of the optical laser field and recombines with the newly formed core vacancy emitting x-ray-boosted HH light.

the liberated electron from the ion is ~ 1 fs for optical laser light. During this time, one may manipulate the cation such that the returning electron sees an altered ion as depicted in Fig. 1. Then, the emitted HH radiation bears the signature of the change. I use resonant x-ray excitation of an inner-shell electron into the transient valence vacancy that is formed by tunnel ionization. The recombination of the returning electron with the core hole leads to a large increase of the energy of the emitted HH light as the energy of the x-ray photons is added to the unmodified HH spectrum. A prerequisite for this to work certainly is that the core hole is not too short lived [94, 95], i.e., it should not decay before the electron returns.

Choosing a geometry of parallel, linear polarization vectors for the optical laser and the x rays, the equations of x-ray-boosted HHG simplify substantially. Namely, as tunnel ionization of valence electrons takes place predominantly along the linear optical laser polarization axis [96–102], mostly the valence states along the polarization axis are depleted which have a magnetic quantum number $m = 0$ which then couple via x rays to core electrons with $m = 0$. In Ref. 80, we examined HHG in krypton atoms where tunnel ionization leads to $4p$ vacancies. There the XUV light is tuned to the $3d \rightarrow 4p$ resonance in the cation which leads to a second high-yield HH plateau that is shifted to higher energies by the XUV photon energy. Similarly, we studied x-ray-boosted HHG for neon $2p$ vacancies where x rays are tuned to the $1s \rightarrow 2p$ resonance in the cation [81]. Both Refs. 80 and 81 focus only on $m = 0$ valence and core states and drop the magnetic quantum number in the notation. If the x rays are very intense, even Rabi flopping [88–93] of the core electron is possible. Such Rabi oscillations have been investigated in neon atoms without optical laser [71, 75, 103–106].

My scheme offers new prospects for HHG involving core electrons, however, if one is only interested in an extension of the HHG cutoff into the kiloelectronvolt regime, one may use conventional HHG that is labora-

tory size and valence-electron based. In this case, the optical laser intensity needs to be high $\sim 10^{15}$ W/cm² and its wavelength should be in the midinfrared instead of the NIR in order to reduce ionization [96–102] to avoid a large electron background that causes phase mismatching. The longer wavelength, however, reduces the efficiency of HHG due to longer continuum propagation and thus enlarged spreading of the wave packet. A good HH yield can, nonetheless, be obtained by a judicious choice of the gas pressure [22, 107–109].

The article is structured as follows. The theory of HHG in the presence of a cw or constant-amplitude optical laser and cw or constant-amplitude x rays, respectively, is developed in Sect. II: I discuss the wave-function ansatz [Sect. II A], the Hamiltonian [Sect. II B], the equations of motion (EOMs) [Sect. II C], the time-dependent dipole transition matrix element [Sect. II D], and the HH spectrum [Sect. II E]. A formalism for a constant-amplitude optical laser and arbitrary x-ray pulses is derived in Sect. III: I specify the Hamiltonian, the wave-function ansatz, and the EOMs [Sect. III A], decouple and integrate the EOMs [Sect. III B], and calculate the time-dependent electric dipole moment and the HH spectrum [Sect. III D]. Conclusions are drawn in Sect. IV. In the Appendices, I discuss the atomic electronic structure, Sect. A, the saddle-point approximation, Sect. B, and the quantum electrodynamic description of HH emission, Sect. C. Accompanying Electronic Supplementary Material [110] is available for this article containing a *Mathematica* [111] Notebook with detailed calculations of a few of the expressions from this article. Atomic units are used throughout [112, 113].

II. HIGH-ORDER HARMONIC GENERATION WITH CONTINUOUS-WAVE X RAYS

I consider HHG for an atom in the two-color light of an optical laser and intense x rays which are both linearly polarized along the z axis and copropagate along the x axis. The optical laser-only problem was treated by Lewenstein *et al.* [12] for a valence electron in SAE [32, 33]. Here I consider also core electrons in addition to valence electrons [Fig. 1]. The combined treatment of HHG and x rays, which may induce Rabi flopping [71, 75, 88–93, 103–106] in the residual ion, represents a genuine two-active-electron problem.

A. Symmetry and basis states

The theory is devised for a closed-shell atom with a spin-singlet ground state. I set out from the nonrelativistic independent-electron approximation for the atomic electronic structure of Hartree-Fock-Slater type [114, 115] with spherical averaging of the one-electron potential leading to a central potential as implemented in the program by Herman and Skillman [116, 117]. Thus, for an

isolated atom without light fields, atomic orbitals with the same principal and angular quantum numbers are degenerate with respect to the magnetic quantum number [118]. As no spin-dependent terms are in the Hamiltonian of the atom in the optical and x-ray light, all quantities can be expressed in terms of spatial atomic orbitals. Consequently, I restrict myself to spatial orbitals occupied by a single electron in the following. Observables, however, need to be multiplied by a factor of two in order to account for the two electrons with opposite spin per spatial orbital.

The essential states necessary to describe HHG in two-color light are deduced as follows. Let the polarization of the optical laser \vec{e}_L and the x rays \vec{e}_X be linear along the z axis, i.e., $\vec{e}_L = \vec{e}_X = \vec{e}_z$ holds. As spin-orbit coupling is not treated which, in any case, only influences strong-field ionization of heavier atoms [119–122], the magnetic quantum number is conserved in the interactions [Appendix A]. Hence, one-electron states of relevance to the problem are the valence states $|a; m_a\rangle$ with magnetic quantum numbers $m_a \in \mathbb{M}_a$ for principal n_a and angular momentum l_a quantum numbers with $\mathbb{M}_a = \{-l_a, \dots, l_a\}$. The core states with n_c and l_c are $|c; m_c\rangle$ for $m_c \in \mathbb{M}_c$ with $\mathbb{M}_c = \{-l_c, \dots, l_c\}$. Continuum states are approximated as free-electron states, i.e., plane waves, and are denoted by $|\vec{k}\rangle$ for $\vec{k} \in \mathbb{R}^3$. Specifically, I use momentum-normalized free-electron wave functions

$$\langle \vec{r} | \vec{k} \rangle = \frac{1}{(2\pi)^{3/2}} e^{i\vec{k}\cdot\vec{r}}, \quad (1)$$

with the position operator \vec{r} [118]. The $|a; m_a\rangle$, $|c; m_c\rangle$, and $|\vec{k}\rangle$ form three classes of one-electron basis states. They are taken to be mutually orthogonal where discrete states are normalized and continuum states are Dirac δ -distribution [123] normalized, i.e., $\langle \vec{k} | \vec{k}' \rangle = \delta^3(\vec{k} - \vec{k}')$. Note that there is a small overlap between continuum states and discrete states which, however, is neglected throughout.

Taking $|\vec{k}\rangle$ for continuum electrons implies that I make the strong-field approximation (SFA) [12], i.e., I neglect the impact of the Coulomb potential of the parent ion on continuum electrons. Only electrons with $m \in \mathbb{M}_2$ for $\mathbb{M}_2 = \mathbb{M}_a \cap \mathbb{M}_c$ are amenable to a core excitation by the x rays with $\vec{e}_X = \vec{e}_z$ in electric dipole approximation [Appendix A] and HHG is modified only for these electrons. For states $|a; m_a\rangle$ with $m_a \in \mathbb{M}_1$ and $\mathbb{M}_1 = \mathbb{M}_a \setminus \mathbb{M}_2$, HHG is described within the SAE approximation [32, 33] following Lewenstein *et al.* [12] because no core electrons couple to these valence vacancies. Hence there are $N/2 = \#\mathbb{M}_a + \#\mathbb{M}_2$ relevant spatial orbitals in the system.

To describe the quantum dynamics of resonant x-ray excitation in the course of HHG, one needs to consider two active electrons: one in the valence or continuum and one in the core or valence. The spatial one-electron states are occupied by two electrons each with opposite spin. To facilitate a core excitation, the spin of

the valence electron liberated by tunnel ionization and the spin of the core electron need to be the same as the interaction with the x rays is spin independent. Whether the valence electron with spin up or spin down is ionized does not change the result and thus it is sufficient to consider only one case [113]. In other words, I need to consider an effective two-electron system formed by one electron from the valence and one electron from the core with the same spin, i.e., the system has triplet spin. The two-electron wave function can be factored into a spin part and a spatial part. Due to the Pauli exclusion principle for indistinguishable particles and the fact that the triplet spin part is symmetric with respect to electron exchange, the spatial part needs to be antisymmetric [113, 118].

I use three different classes of two-electron basis states. First, the ground state of the two-electron system for $m \in \mathbb{M}_2$ is given by the Slater determinant

$$|a c; m\rangle = \frac{1}{\sqrt{2}} [|a; m\rangle \otimes |c; m\rangle - |c; m\rangle \otimes |a; m\rangle]. \quad (2)$$

This is a normalized linear combination of tensorial products of the two respective one-electron states which is antisymmetric with respect to electron exchange; it incorporates probabilistic correlations between electrons [91, 113]. As core states are energetically separated from valence states, electron correlations due to Coulomb interaction between core and valence electrons beyond the Hartree-Fock-Slater approximation [114, 115] are small and neglecting them has a minor influence on excitation and ionization energies which is referred to as core-valence separation [124, 125].

Second, the valence-excited states with one electron in the continuum for $\vec{k} \in \mathbb{R}^3$ and one electron in the core with $m \in \mathbb{M}_2$ are

$$|\vec{k} c; m\rangle = \frac{1}{\sqrt{2}} [|\vec{k}\rangle \otimes |c; m\rangle - |c; m\rangle \otimes |\vec{k}\rangle]. \quad (3)$$

Third, the core-excited states with one electron in the continuum, $\vec{k} \in \mathbb{R}^3$, and one electron in the valence state, $m \in \mathbb{M}_2$, are

$$|\vec{k} a; m\rangle = \frac{1}{\sqrt{2}} [|\vec{k}\rangle \otimes |a; m\rangle - |a; m\rangle \otimes |\vec{k}\rangle]. \quad (4)$$

Note that in Refs. 80 and 81, Hartree products are used for the three classes of two-electron basis states (2), (3), and (4) instead of Slater determinants. This does not cause any difficulties as long as the two-electron dipole operator is defined suitably—Eqs. (39), (40) restricted to two electrons—such that it leads to Eq. (5) of Ref. 80.

From the one- and two-electron basis states of the previous two paragraphs, I construct the ground state $|\Phi_0\rangle$ and the valence-excited $|\Phi_{\vec{k}c}^{(m)}\rangle$ and core-excited $|\Phi_{\vec{k}a}^{(m)}\rangle$ states of the $N/2$ electron system for $m \in \mathbb{M}_2$. If $\mathbb{M}_1 \neq \emptyset$, then I need to include those one-electron valence-excited states which do not couple via x rays to core electrons $|\Phi_{\vec{k}}^{(m)}\rangle$ for $m \in \mathbb{M}_1$. For $l_a = l_c + 1$, this gives

rise to a left $|\Phi_L\rangle = |a; -l_a\rangle$, and a right $|\Phi_R\rangle = |a; l_a\rangle$ valence state. Then, the $N/2$ electron ground state of the atom is given for $l_a = l_c + 1$ by

$$|\Phi_0\rangle = \frac{1}{\sqrt{\#\mathbb{M}_a}} |\Phi_L\rangle \otimes \left[\bigotimes_{m=\min \mathbb{M}_2}^{\max \mathbb{M}_2} |a c; m\rangle \right] \otimes |\Phi_R\rangle. \quad (5)$$

For $l_a = l_c - 1$, I have $\mathbb{M}_1 = \emptyset$ and I omit the factors $|\Phi_L\rangle$ and $|\Phi_R\rangle$. Here $\#\mathbb{M}_a$ stands for the number of elements in the set \mathbb{M}_a . From the ground state (5), I form valence-excited states $|\Phi_{\vec{k}c}^{(m)}\rangle$ for $m \in \mathbb{M}_2$ by replacing $|a c; m\rangle$ [Eq. (2)] with $|\vec{k}c; m\rangle$ [Eq. (3)] for $\vec{k} \in \mathbb{R}^3$. For $l_a = l_c + 1$, I additionally have the valence-excited states $|\Phi_{\vec{k}}^{(-l_a)}\rangle$ and $|\Phi_{\vec{k}}^{(l_a)}\rangle$ by substituting $|\Phi_L\rangle$ or $|\Phi_R\rangle$ in Eq. (5) by $|\vec{k}\rangle$, respectively; otherwise, for $l_a = l_c - 1$, the extra factors are left out. Finally, core-excited states $|\Phi_{\vec{k}a}^{(m)}\rangle$ for $m \in \mathbb{M}_2$ are constructed from Eq. (5) by replacing $|a c; m\rangle$ [Eq. (2)] with $|\vec{k}a; m\rangle$ [Eq. (4)] for $\vec{k} \in \mathbb{R}^3$.

In summary, I apply the three assumptions of Lewenstein *et al.* from page 2119 of Ref. 12 in a somewhat modified way where I need to account for the interaction with x rays in the parent ion by adding clauses:

- (a) The bound one-electron states of the system are the valence states $|a; m_a\rangle$ with $m_a \in \mathbb{M}_a$ and the core states $|c; m_c\rangle$ with $m_c \in \mathbb{M}_2$.
- (b) Continuum electrons are described as free electrons $|\vec{k}\rangle$ for $\vec{k} \in \mathbb{R}^3$ [Eq. (1)] and, consequently, the influence of the Coulomb potential of the residual ion is omitted.
- (c) The system is completely described by the three classes of $N/2$ electron states: the atomic ground state $|\Phi_0\rangle$, the valence-excited states $|\Phi_{\vec{k}}^{(m_1)}\rangle$ for $m_1 \in \mathbb{M}_1$, $|\Phi_{\vec{k}c}^{(m_2)}\rangle$ for $m_2 \in \mathbb{M}_2$, and the core-excited states $|\Phi_{\vec{k}a}^{(m_2)}\rangle$, which are formed using the one-electron states from (a) and (b), and $\vec{k} \in \mathbb{R}^3$.
- (d) Continuum-continuum transitions are only considered for the interaction of a continuum electron with the optical laser and do not play a role anywhere else.
- (e) The coherent interaction of x rays with the atom—where the photon energy is tuned in resonance with the core-valence level spacing—is confined to the two-level systems formed by $|\Phi_{\vec{k}c}^{(m)}\rangle$ and $|\Phi_{\vec{k}a}^{(m)}\rangle$ for $m \in \mathbb{M}_2$ and $\vec{k} \in \mathbb{R}^3$.
- (f) The depopulation of the states $|\Phi_0\rangle$, $|\Phi_{\vec{k}}^{(m_1)}\rangle$ for $m_1 \in \mathbb{M}_1$, $|\Phi_{\vec{k}c}^{(m_2)}\rangle$ and $|\Phi_{\vec{k}a}^{(m_2)}\rangle$ for $m_2 \in \mathbb{M}_2$ with $\vec{k} \in \mathbb{R}^3$ by optical laser-induced and x-ray-induced ionization is represented by phenomenological destruction rates $\Gamma'_i(t)$ for $i \in \{0, a, c\}$ where

$\Gamma'_c(t)$ also accounts for core-hole decay. The destruction rates $\Gamma'_i(t)$ are assumed to be independent of m_1 , m_2 , and \vec{k} .

- (g) A single HH photon is emitted in HHG whereby HH emission due to transitions to the ground state occurs. For a complete description, I need the vacuum photon state and the single HH photon number states. Propagation of HH light is along the x axis.

Point (e) is justified by the fact that x rays oscillate very rapidly and cause only a small ponderomotive potential [126, 127]. Ionization of $|\Phi_{\vec{k}}^{(m_1)}\rangle$, $|\Phi_{\vec{k}c}^{(m_2)}\rangle$, and $|\Phi_{\vec{k}a}^{(m_2)}\rangle$ by the optical laser is much smaller in point (f) than for the neutral atom as the ionization potential of the cation is significantly larger than the ionization potential of the neutral atom and the tunneling rate depends exponentially on the ionization potential [96–102]. In point (f), ionization by the x rays and the optical laser is treated incoherently via phenomenological destruction rates in contrast to the coherent formulation of resonant x-ray absorption in point (e).

The phenomenological destruction rates of point (f) are determined following Ref. 82. I assume approximately monochromatic x rays, i.e., the photoabsorption cross sections σ_0 , σ_a , and σ_c for one-x-ray-photon absorption by the atom in the ground state, valence-excited and core-excited states, respectively, can be obtained with Refs. 128 and 129 and are approximately constant over the bandwidth of the x-ray pulse that has a central angular frequency ω_X . Further, the x-ray intensity is represented by $I_X(t)$ implying an x-ray photon flux of $J_X(t) \approx \frac{I_X(t)}{\omega_X}$. With the tunneling rates $\Gamma_{L,0}(t)$, $\Gamma_{L,a}(t)$, and $\Gamma_{L,c}(t)$ induced by the optical laser [96–102], the instantaneous phenomenological destruction rates of the atom in the three classes of basis states are given by

$$\Gamma'_i(t) = \Gamma_{L,i}(t) + \sigma_i J_X(t) + \delta_{i,c} \gamma_c, \quad (6)$$

for $i \in \{0, a, c\}$ [82] with the intrinsic decay width γ_c from Auger and radiative decay of the core-excited state [94, 95] and $\delta_{i,c}$ is the Kronecker- δ [123]. *Nota bene*, that I omitted the dependence of $\Gamma_{L,i}(t)$ for $i \in \{a, c\}$ on the magnetic quantum number [96–102]. This is justified as there is only a single ground state with $\Gamma_{L,0}(t)$ and destruction by the optical laser is strongly suppressed for the parent ion. For cw light, I determine time-independent destruction rates by averaging $\Gamma'_i(t)$ from Eq. (6) over an optical laser cycle

$$\Gamma_i = \frac{1}{T_L} \int_0^{T_L} \Gamma'_i(t) dt'. \quad (7)$$

B. Hamiltonian

The total $N/2$ -electron Hamiltonian of the atom in two-color light (optical laser and x rays) reads

$$\hat{H} = \hat{H}_A + \hat{H}_L + \hat{H}_X ; \quad (8)$$

it consist of three parts: the atomic electronic structure \hat{H}_A , the interaction with the optical laser \hat{H}_L , and the interaction with the x rays \hat{H}_X .

The one-electron Hamiltonian for the atomic electronic structure is

$$\begin{aligned} \hat{h}_A = & \sum_{m \in \mathbb{M}_a} |a; m\rangle \varepsilon_a \langle a; m| + \sum_{m \in \mathbb{M}_2} |c; m\rangle \varepsilon_c \langle c; m| \\ & + \int_{\mathbb{R}^3} |\vec{k}\rangle \frac{\vec{k}^2}{2} \langle \vec{k}| d^3k , \end{aligned} \quad (9)$$

with the energies $\varepsilon_a, \varepsilon_c$, and $\frac{\vec{k}^2}{2}$ of the one-electron states. The $N/2$ -electron atomic electronic structure Hamiltonian follows to

$$\begin{aligned} \hat{H}_A = & \sum_{i=1}^{N/2} \hat{\mathbb{1}}_{\text{el}}^{i-1} \otimes \hat{h}_A \otimes \hat{\mathbb{1}}_{\text{el}}^{N/2-i} - i |\Phi_0\rangle \frac{\Gamma_0}{2} \langle \Phi_0| \\ & - i \sum_{m \in \mathbb{M}_1} \int_{\mathbb{R}^3} |\Phi_{\vec{k}}^{(m)}\rangle \frac{\Gamma_a}{2} \langle \Phi_{\vec{k}}^{(m)}| d^3k \quad (10) \\ & - i \sum_{m \in \mathbb{M}_2} \int_{\mathbb{R}^3} [|\Phi_{\vec{k}c}^{(m)}\rangle \frac{\Gamma_a}{2} \langle \Phi_{\vec{k}c}^{(m)}| \\ & + |\Phi_{\vec{k}a}^{(m)}\rangle \frac{\Gamma_c}{2} \langle \Phi_{\vec{k}a}^{(m)}|] d^3k , \end{aligned}$$

with the unity operator in the one-electron Hilbert space $\hat{\mathbb{1}}_{\text{el}}$ and the time-independent destruction rates (7).

The interaction of a single electron with the optical laser field is described in electric dipole approximation in length form [92] by

$$\begin{aligned} \hat{h}_L = & E_L(t) \sum_{m \in \mathbb{M}_a} \int_{\mathbb{R}^3} [|\vec{k}\rangle \langle \vec{k}| \vec{e}_L \cdot \vec{r} |a; m\rangle \\ & \times \langle a; m| + \text{h.c.}] d^3k \quad (11) \\ & + E_L(t) \int_{\mathbb{R}^3} \int_{\mathbb{R}^3} |\vec{k}\rangle \langle \vec{k}| \vec{e}_L \cdot \vec{r} |\vec{k}'\rangle \langle \vec{k}'| d^3k d^3k' . \end{aligned}$$

With ‘‘h.c.’’ I denote the Hermitian conjugate of the preceding summand and I use the electric field of the optical laser

$$E_L(t) = E_{0L} \cos(\omega_L t) , \quad (12)$$

with the peak amplitude E_{0L} and the angular frequency ω_L [92, 93, 117]. The $N/2$ -electron Hamiltonian for the interaction with the optical laser reads

$$\hat{H}_L = \sum_{i=1}^{N/2} \hat{\mathbb{1}}_{\text{el}}^{i-1} \otimes \hat{h}_L \otimes \hat{\mathbb{1}}_{\text{el}}^{N/2-i} . \quad (13)$$

The optical laser couples only valence electrons to the continuum; the coupling of core electrons to the continuum by the optical laser is negligible. The influence of the optical laser on continuum electrons is represented by the last term on the right hand side of Eq. (11).

The interaction of a single electron with the x-ray radiation is described in electric dipole approximation in length form [92] via

$$\hat{h}_X = E_X(t) \sum_{m \in \mathbb{M}_2} [|c; m\rangle \langle c; m| \vec{e}_X \cdot \vec{r} |a; m\rangle \langle a; m| + \text{h.c.}] , \quad (14)$$

for the x-ray electric field

$$E_X(t) = E_{0X} \cos(\omega_X t) = \frac{E_{0X}}{2} [e^{i\omega_X t} + e^{-i\omega_X t}] , \quad (15)$$

with the peak amplitude E_{0X} and the angular frequency ω_X [92, 93, 117]. The $N/2$ -electron Hamiltonian for the x-ray interaction follows similarly as in Eq. (13) to

$$\hat{H}_X = \sum_{i=1}^{N/2} \hat{\mathbb{1}}_{\text{el}}^{i-1} \otimes \hat{h}_X \otimes \hat{\mathbb{1}}_{\text{el}}^{N/2-i} . \quad (16)$$

C. Equations of motion

I make the following ansatz for the $N/2$ -electron wave packet

$$\begin{aligned} |\Psi, t\rangle = & a(t) e^{-iE_0 t} |\Phi_0\rangle \\ & + \sum_{m \in \mathbb{M}_1} \int_{\mathbb{R}^3} b_a^{(m)}(\vec{k}, t) e^{-iE_0 t} |\Phi_{\vec{k}}^{(m)}\rangle d^3k \quad (17) \\ & + \sum_{m \in \mathbb{M}_2} \int_{\mathbb{R}^3} [b_a^{(m)}(\vec{k}, t) e^{-iE_0 t} |\Phi_{\vec{k}c}^{(m)}\rangle \\ & + b_c^{(m)}(\vec{k}, t) e^{-i(E_0 + \omega_X) t} |\Phi_{\vec{k}a}^{(m)}\rangle] d^3k . \end{aligned}$$

The subscripts ‘‘a’’ and ‘‘c’’ on the amplitudes $b_a^{(m)}(\vec{k}, t)$ and $b_c^{(m)}(\vec{k}, t)$, respectively, indicate which one-electron state contains the hole. The ground-state energy of the atom is $E_0 = \langle \Phi_0 | \hat{H}_A | \Phi_0 \rangle + i \frac{\Gamma_0}{2} = \#\mathbb{M}_a \varepsilon_a + \#\mathbb{M}_2 \varepsilon_c$. The phase factors in the ansatz (17) are chosen such that the equations of motion (EOMs), which are derived in the following, are simplified the most, that fast oscillations are separated, and thus the expansion coefficients $a(t)$, $b_a^{(m)}(\vec{k}, t)$, and $b_c^{(m)}(\vec{k}, t)$ vary comparatively slowly. I insert $|\Psi, t\rangle$ from Eq. (17) into the time-dependent Schrödinger equation [118] yielding

$$i \frac{\partial}{\partial t} |\Psi, t\rangle = \hat{H} |\Psi, t\rangle , \quad (18)$$

with the Hamiltonian from Eq. (8). I project onto the three classes of basis states from Sect. II A which yields EOMs for the expansion coefficients in Eq. (17).

First, I obtain the EOM for the ground-state amplitude by projecting onto $\langle \Phi_0 |$ giving

$$\frac{d}{dt} a(t) = -\frac{\Gamma_0}{2} a(t) - i \sum_{m \in \mathbb{M}_a} \int_{\mathbb{R}^3} \langle a; m | \hat{h}_L | \vec{k} \rangle b_a^{(m)}(\vec{k}, t) d^3 k. \quad (19)$$

The second term on the right-hand side is the rate of change of the ground-state amplitude due to tunnel ionization of a valence electron induced by the optical laser and recombination of a continuum electron with the valence vacancy. As the efficiency of HHG is low, tunnel ionization is the only noticeable contribution; it can be neglected entirely for low ground-state depopulation by the optical laser [12]. For high depopulation, the influence of the second term on the right-hand side of Eq. (19) is included in Γ_0 as in Eqs. (6) and (7). Consequently, the term is dropped in Eq. (19) [12, 82].

The Eq. (19) becomes identical to Eq. (49) of Ref. 12 upon dropping the first term on the right-hand side, setting $M_a = \{0\}$ and replacing $\langle a; m | \hat{h}_L | \vec{k} \rangle \rightarrow -E \cos(t) d_x^*(\mathbf{v})$, $b_a^{(m)}(\vec{k}, t) \rightarrow b(\mathbf{v}, t)$, and $\vec{k} \rightarrow \mathbf{v}$.

Second, projecting onto $\langle \Phi_{\vec{k}c}^{(m)} |$ for $\vec{k} \in \mathbb{R}^3$ and $m \in \mathbb{M}_2$ [Eq. (3)] gives the EOMs for a continuum electron and a valence hole where the valence hole is coupled to core electrons:

$$\begin{aligned} \frac{\partial}{\partial t} b_a^{(m)}(\vec{k}, t) &= -\frac{i}{2} (\vec{k}^2 - \delta + 2\mathcal{I}_p - i\Gamma_a) b_a^{(m)}(\vec{k}, t) \\ &\quad - i \int_{\mathbb{R}^3} \langle \vec{k} | \hat{h}_L | \vec{k}' \rangle b_a^{(m)}(\vec{k}', t) d^3 k' \\ &\quad - i \langle c; m | \hat{h}_{X,RWA} | a; m \rangle b_c^{(m)}(\vec{k}, t) \\ &\quad - i \langle \vec{k} | \hat{h}_L | a; m \rangle a(t). \end{aligned} \quad (20)$$

The first term on the right-hand side of Eq. (20) specifies the phase of $b_a^{(m)}(\vec{k}, t)$. Following Refs. 80 and 81, I introduce the energy

$$\mathcal{I}_p = -\frac{1}{2} (\varepsilon_a + \varepsilon_c + \omega_x) = -\varepsilon_a + \frac{\delta}{2} \quad (21)$$

and the detuning [93] of the x-ray photon energy from the energy difference between the core and valence levels

$$\delta = \varepsilon_a - \varepsilon_c - \omega_x. \quad (22)$$

For zero detuning, \mathcal{I}_p corresponds to the valence ionization potential of the atom, but \mathcal{I}_p is shifted to higher (lower) values, if ω_x is smaller (larger) than the level spacing. The second term on the right-hand side of Eq. (20) describes optical-laser-mediated continuum-continuum transitions; the third term stands for resonant excitation by the x rays, where I make the rotating wave approximation $\hat{h}_X e^{-i\omega_x t} \approx \hat{h}_{X,RWA}$ [92, 93]; and the fourth term induces tunnel ionization.

Similarly, projecting onto $\langle \Phi_{\vec{k}}^{(m)} |$ for $\vec{k} \in \mathbb{R}^3$ and $m \in \mathbb{M}_1$ gives the EOMs for the recombination of the

continuum electron when there is no coupling to core electrons. The resulting EOMs are the same as Eq. (20) apart from the term $-i b_c^{(m)}(\vec{k}, t) \langle c; m | \hat{h}_{X,RWA} | a; m \rangle$ which is missing in this case. These EOMs contribute only to optical-laser HHG with valence electrons.

Third, projecting onto $\langle \Phi_{\vec{k}a}^{(m)} |$ for $\vec{k} \in \mathbb{R}^3$ and $m \in \mathbb{M}_2$ provides the EOMs for a continuum electron and a core hole

$$\begin{aligned} \frac{\partial}{\partial t} b_c^{(m)}(\vec{k}, t) &= -\frac{i}{2} (\vec{k}^2 + \delta + 2\mathcal{I}_p - i\Gamma_c) b_c^{(m)}(\vec{k}, t) \\ &\quad - i \int_{\mathbb{R}^3} \langle \vec{k} | \hat{h}_L | \vec{k}' \rangle b_c^{(m)}(\vec{k}', t) d^3 k' \\ &\quad - i \langle a; m | \hat{h}_{X,RWA} | c; m \rangle b_a^{(m)}(\vec{k}, t). \end{aligned} \quad (23)$$

The tunnel ionization rate of core electrons is vanishingly small such that the last term on the right-hand side of Eq. (20) is missing here.

In order to evaluate the matrix elements in the EOMs that involve continuum electrons (20), (23), I use the spatial part of the free-electron wave function of Eq. (1). Specifically, I obtain from Eqs. (11) and (12) the matrix element that is responsible for tunnel ionization of the valence state

$$\langle \vec{k} | \hat{h}_L | a; m \rangle = E_L(t) \wp_{L,\vec{k}a}^{(m)}, \quad (24)$$

with $\wp_{L,\vec{k}a}^{(m)} = \langle \vec{k} | \vec{e}_L \cdot \vec{r} | a; m \rangle$ [Appendix A 2]. Optical laser-induced continuum-continuum transitions [12] are described by the matrix element [Appendix A 3]:

$$\langle \vec{k} | \hat{h}_L | \vec{k}' \rangle = E_L(t) (-i) \frac{\partial}{\partial k'_z} \delta^3(\vec{k}' - \vec{k}). \quad (25)$$

Further, x-ray transitions in Eqs. (20) and (23) are described by

$$\langle c; m | \hat{h}_{X,RWA} | a; m \rangle = \frac{E_{0X}}{2} \wp_{X,ca}^{(m)} = \frac{R_{0X}^{(m)}}{2} \quad (26)$$

using Eqs. (14) and (15) with $\wp_{X,ca}^{(m)} = \langle c; m | \vec{e}_X \cdot \vec{r} | a; m \rangle$ [Appendix A 1] and defining the real Rabi frequency $R_{0X}^{(m)}$ [92, 93]. I choose the spatial matrix element $\wp_{X,ca}^{(m)}$ and thus $R_{0X}^{(m)}$ to be real which is feasible as the atomic potential is approximated by a central potential [116, 117].

I rewrite Eqs. (20) and (23) as a vector equation for $\vec{k} \in \mathbb{R}^3$ and $m \in \mathbb{M}_2$ defining the continuum-electron amplitudes

$$\vec{b}^{(m)}(\vec{k}, t) \equiv (b_a^{(m)}(\vec{k}, t), b_c^{(m)}(\vec{k}, t))^T \quad (27)$$

and the complex symmetric Rabi matrix

$$\mathbf{R}^{(m)} = \begin{pmatrix} -\delta - i\Gamma_a & R_{0X}^{(m)} \\ R_{0X}^{(m)} & \delta - i\Gamma_c \end{pmatrix}. \quad (28)$$

This yields, with Eqs. (25) and (26), the combined EOMs for a continuum electron with either a valence hole or a core hole

$$\begin{aligned} \frac{\partial}{\partial t} \vec{b}^{(m)}(\vec{k}, t) &= -\frac{i}{2} (\mathbf{R}^{(m)} + (\vec{k}^2 + 2\mathcal{I}_P) \mathbb{1}) \vec{b}^{(m)}(\vec{k}, t) \\ &+ E_L(t) \frac{\partial}{\partial k_z} \vec{b}^{(m)}(\vec{k}, t) \\ &- i E_L(t) \varphi_{L, \vec{k}a}^{(m)} \begin{pmatrix} 1 \\ 0 \end{pmatrix} a(t). \end{aligned} \quad (29)$$

The matrix of eigenvalues of $\mathbf{R}^{(m)}$ is

$$\mathbf{\Lambda}^{(m)} = \text{diag}(\lambda_+^{(m)}, \lambda_-^{(m)}) \quad (30)$$

with the eigenvalues [110]:

$$\lambda_{\pm}^{(m)} = -\frac{i}{2} (\Gamma_a + \Gamma_c) \pm \mu^{(m)}, \quad (31)$$

and the complex Rabi frequency [93] given by

$$\mu^{(m)} = \sqrt{[\delta + \frac{i}{2} (\Gamma_a - \Gamma_c)]^2 + (R_{0X}^{(m)})^2}. \quad (32)$$

The matrix of eigenvectors of $\mathbf{R}^{(m)}$ is denoted by $\mathbf{U}^{(m)}$. With the eigenvectors $\mathbf{U}^{(m)}$ and eigenvalues $\mathbf{\Lambda}^{(m)}$, I transform to the eigenbasis of $\mathbf{R}^{(m)}$, the x-ray-dressed states [93]. With Eq. (27), I find the new amplitudes

$$\vec{\mathfrak{b}}^{(m)}(\vec{k}, t) \equiv \begin{pmatrix} \mathfrak{b}_+^{(m)}(\vec{k}, t) \\ \mathfrak{b}_-^{(m)}(\vec{k}, t) \end{pmatrix} = (\mathbf{U}^{(m)})^{-1} \vec{b}^{(m)}(\vec{k}, t) \quad (33)$$

and define the valence ionization fraction by

$$\vec{w}^{(m)} \equiv \begin{pmatrix} w_+^{(m)} \\ w_-^{(m)} \end{pmatrix} = (\mathbf{U}^{(m)})^{-1} \begin{pmatrix} 1 \\ 0 \end{pmatrix}. \quad (34)$$

Next, I recast Eq. (29) in terms of x-ray-dressed states with Eqs. (30), (33), (34), leading to

$$\begin{aligned} \frac{\partial}{\partial t} \vec{\mathfrak{b}}^{(m)}(\vec{k}, t) &= -\frac{i}{2} (\mathbf{\Lambda}^{(m)} + (\vec{k}^2 + 2\mathcal{I}_P) \mathbb{1}) \vec{\mathfrak{b}}^{(m)}(\vec{k}, t) \\ &+ E_L(t) \frac{\partial}{\partial k_z} \vec{\mathfrak{b}}^{(m)}(\vec{k}, t) \\ &- i E_L(t) \varphi_{L, \vec{k}a}^{(m)} \vec{w}^{(m)} a(t), \end{aligned} \quad (35)$$

where I exploit that $\mathbf{U}^{(m)}$ neither depends on \vec{k} nor on t and thus commutes with derivatives with respect to both variables.

Equation (35) is a system of two decoupled partial differential equations. To transform it into two ordinary differential equations, I introduce the vector potential [126, 127] of the optical laser

$$\begin{aligned} \vec{A}_L(t) &= - \lim_{\eta \rightarrow 0^+} \int_{-\infty}^t E_L(t') \vec{e}_L e^{-\eta|t'|} dt' \\ &= - \frac{E_{0L}}{\omega_L} \sin(\omega_L t) \vec{e}_L, \end{aligned} \quad (36)$$

which is determined from its electric field (12). The factor $e^{-i\eta|t'|}$ with $\eta > 0$, thereby, ensures convergence of the integral [130]. As the kinetic momentum of the continuum electron \vec{k} at time t in Eq. (35) can be expressed at time t' by $\vec{k}' = \vec{k} - \vec{A}_L(t) + \vec{A}_L(t')$ [12], the sum of the left hand side of Eq. (35) and the negative of the summand on the right hand side that contains the derivative with respect to k_z' represents a total time derivative of $\vec{\mathfrak{b}}(\vec{k}', t')$ with respect to t' and I have

$$\begin{aligned} \frac{d}{dt'} \vec{\mathfrak{b}}^{(m)}(\vec{k}', t') &= -\frac{i}{2} [\mathbf{\Lambda}^{(m)} + 2\mathcal{I}_P \mathbb{1} \\ &+ (\vec{k} - \vec{A}_L(t) + \vec{A}_L(t'))^2 \mathbb{1}] \\ &\times \vec{\mathfrak{b}}^{(m)}(\vec{k}', t') \\ &- i E_L(t') \varphi_{L, \vec{k} - \vec{A}_L(t) + \vec{A}_L(t') a}^{(m)} \\ &\times \vec{w}^{(m)} a(t'). \end{aligned} \quad (37)$$

This is a system of two ordinary first-order differential equations which can be integrated exactly [123] yielding

$$\begin{aligned} \mathfrak{b}_{\pm}^{(m)}(\vec{k}, t) &= -i w_{\pm}^{(m)} \int_0^t E_L(t') \varphi_{L, \vec{k} - \vec{A}_L(t) + \vec{A}_L(t') a}^{(m)} \\ &\times e^{-\frac{i}{2} \int_{t'}^t (\vec{k} - \vec{A}_L(t) + \vec{A}_L(t''))^2 dt''} \\ &\times e^{-i(\frac{\lambda_{\pm}^{(m)}}{2} + \mathcal{I}_P)(t-t')} a(t') dt', \end{aligned} \quad (38)$$

by letting $t' = t$ in the solution of Eq. (37) because then $\vec{k}' = \vec{k}$ and thus $\mathfrak{b}_{\pm}(\vec{k}, t) = \mathfrak{b}_{\pm}(\vec{k}', t')$. Next, I transform back to the amplitudes of the bare states (33) via $\vec{b}^{(m)}(\vec{k}, t) = \mathbf{U}^{(m)} \vec{\mathfrak{b}}^{(m)}(\vec{k}, t)$ providing the solution of Eq. (29).

The EOMs for $m \in \mathbb{M}_1$ follow from Eq. (38) by the replacements $\mathfrak{b}_{\pm}^{(m)}(\vec{k}, t) \rightarrow b_a^{(m)}(\vec{k}, t)$, $w_{\pm}^{(m)} \rightarrow 1$, and $\lambda_{\pm}^{(m)} \rightarrow -\delta - i\Gamma_a$.

To transform Eq. (38) into Eq. (5) of Lewenstein *et al.* [12], I make the replacements $\mathfrak{b}_{\pm}^{(m)}(\vec{k}, t) \rightarrow b(\mathbf{v}, t)$, $-i w_{\pm}^{(m)} \rightarrow i$, $\varphi_{L, \vec{k} - \vec{A}_L(t) + \vec{A}_L(t') a}^{(m)} \rightarrow d_x(\mathbf{v} + \mathbf{A}(t) - \mathbf{A}(t'))$, $\vec{A}_L \rightarrow -\mathbf{A}$, $E_L(t') \rightarrow E \cos t'$, and $\frac{\lambda_{\pm}^{(m)}}{2} + \mathcal{I}_P \rightarrow I_P$.

D. Electric dipole transition matrix element

The emission of HH light in electric dipole approximation is governed by the position operator \vec{r} projected onto the polarization vector of the emitted HH light \vec{e}_H , i.e., the one-electron dipole operator is $\hat{d}_1 = \vec{e}_H \cdot \vec{r}$ [92, 93]. Furthermore, the two-electron dipole operator is $\hat{D}_2 = \hat{d}_1 \otimes \hat{1}_{el} + \hat{1}_{el} \otimes \hat{d}_1$. With this, the $N/2$ -electron dipole operator, in terms of the basis states from Sect. II A, fol-

lows to

$$\begin{aligned} \hat{D} = & \sum_{m \in \mathbb{M}_1} \int_{\mathbb{R}^3} |\Phi_0\rangle \langle a; m | \hat{d}_1 | \vec{k} \rangle \langle \Phi_{\vec{k}}^{(m)} | d^3k + \text{h.c.} \\ & + \sum_{m \in \mathbb{M}_2} \int_{\mathbb{R}^3} [|\Phi_0\rangle \langle a; c; m | \hat{D}_2 | \vec{k}; c; m \rangle \langle \Phi_{\vec{k}; c}^{(m)} | \\ & + |\Phi_0\rangle \langle a; c; m | \hat{D}_2 | \vec{k}; a; m \rangle \langle \Phi_{\vec{k}; a}^{(m)} |] d^3k + \text{h.c.} . \end{aligned} \quad (39)$$

The operator \hat{D} in Eq. (39) is defined such that it describes the recombination of a continuum electron with valence and core holes [131]. For $\vec{k} \in \mathbb{R}^3$, the one-electron dipole matrix elements are $\varphi_{\text{H},a\vec{k}}^{(m)} = \langle a; m | \hat{d}_1 | \vec{k} \rangle$ with $m \in \mathbb{M}_1$ whereas the two-electron dipole matrix elements are $\varphi_{\text{H},a\vec{k}}^{(m)} = \langle a; c; m | \hat{D}_2 | \vec{k}; c; m \rangle$ and $\varphi_{\text{H},c\vec{k}}^{(m)} = -\langle a; c; m | \hat{D}_2 | \vec{k}; a; m \rangle$ with $m \in \mathbb{M}_2$.

High-order harmonic emission is determined by the time-dependent dipole transition matrix element between the atomic ground state and the valence-excited and core-excited states, respectively. Namely, it is expressed by $\mathcal{D}(t) = \langle \Psi_0, t | \hat{D} | \Psi_c, t \rangle$ where $|\Psi_0, t\rangle$ is the ground-state part of the wave packet (17) at time t and $|\Psi_c, t\rangle$ is the continuum part [14]. Then, the dipole transition matrix element follows from Eqs. (17) and (39) to

$$\begin{aligned} \mathcal{D}(t) = & a_0^*(t) \int_{\mathbb{R}^3} \left[\sum_{m \in \mathbb{M}_a} \varphi_{\text{H},a\vec{k}}^{(m)} b_a^{(m)}(\vec{k}, t) \right. \\ & \left. - \sum_{m \in \mathbb{M}_2} \varphi_{\text{H},c\vec{k}}^{(m)} e^{-i\omega_X t} b_c^{(m)}(\vec{k}, t) \right] d^3k \\ = & \sum_{m \in \mathbb{M}_1} \mathfrak{d}^{(m)}(t) + \sum_{m \in \mathbb{M}_2} \sum_{\substack{i \in \{a,c\} \\ j \in \{+,-\}}} \mathfrak{D}_{ij}^{(m)}(t) . \end{aligned} \quad (40)$$

The dipole components, with $m \in \mathbb{M}_2$, for the valence- and the core-excited states, $i \in \{a, c\}$, and the x-ray-dressed states, $j \in \{+, -\}$, are introduced by

$$\begin{aligned} \mathfrak{D}_{ij}^{(m)}(t) = & (-1)^{\delta_{i,c}} U_{ij}^{(m)} e^{-i\delta_{i,c}\omega_X t} a_0^*(t) \\ & \times \int_{\mathbb{R}^3} \varphi_{\text{H},i\vec{k}}^{(m)} \mathfrak{b}_j^{(m)}(\vec{k}, t) d^3k \\ = & (-1)^{\delta_{i,c}} (-i) U_{ij}^{(m)} w_j^{(m)} e^{-i\delta_{i,c}\omega_X t} a^*(t) \\ & \times \int_0^t a(t') E_L(t') \int_{\mathbb{R}^3} \varphi_{\text{H},\vec{p}+\vec{A}_L(t)}^{(m)*} \varphi_{\text{L},\vec{p}+\vec{A}_L(t')}^{(m)} \\ & \times e^{-iS_j^{(m)}(\vec{p},t,t')} d^3p dt' . \end{aligned} \quad (41)$$

Here I inserted the amplitudes of Eq. (38) transformed from the x-ray-dressed-state basis back to the bare-state basis via $U_{ij}^{(m)}$. The Kronecker $\delta_{i,c}$ [123] is used to insert the phase factor $e^{-i\omega_X t}$ for the terms involving core-excited states. I also introduced the canonical momen-

tum [132] $\vec{p} = \vec{k} - \vec{A}_L(t)$ and the quasiclassical action

$$S_j^{(m)}(\vec{p}, t, t') = \frac{1}{2} \int_{t'}^t (\vec{p} + \vec{A}_L(t''))^2 dt'' + \left(\frac{\lambda_j^{(m)}}{2} + \mathcal{I}_P \right) (t - t') . \quad (42)$$

Equation (41) can be understood term by term [12]. Namely, $w_j^{(m)} \varphi_{\text{L},\vec{p}+\vec{A}_L(t')}^{(m)} E_L(t')$ determines valence ionization at time t' via tunneling in the optical laser field. During propagation of the free electron from time t' to t in the optical laser field, the electron acquires the phase $e^{-iS_j^{(m)}(\vec{p},t,t')}$. The emission of HH light at time t due to recombination of the free electron with the state $i \in \{a, c\}$ is governed by $\varphi_{\text{H},\vec{p}+\vec{A}_L(t)}^{(m)*}$; the shift of the HH spectrum by ω_X for a recombination with a core hole is given by $e^{-i\delta_{i,c}\omega_X t}$. The quasiclassical action (42) differs from the optical laser-only case [12] by the summand $\left(\frac{\lambda_j^{(m)}}{2} + \mathcal{I}_P - I_P \right) (t - t')$ which represents the energy splitting of the core and valence states due to x-ray dressing.

Equation (42) is the same as Eq. (9) in Ref. 12 after replacing $\vec{p} + \vec{A}_L(t'') \rightarrow \mathbf{p} - \mathbf{A}(t'')$ and $\frac{\lambda_j^{(m)}}{2} + \mathcal{I}_P \rightarrow I_P$.

To calculate $\mathcal{D}(t)$ [Eq. (40)], I make the saddle-point approximation [Appendix B] for the integration over the canonical momentum \vec{p} in Eq. (41). The stationary points [133] of $S_j^{(m)}(\vec{p}, t, t')$ [Eq. (42)] are determined from $\vec{\nabla}_{\vec{p}} S_j^{(m)}(\vec{p}, t, t') = \vec{0} = \vec{s}(t) - \vec{s}(t')$ which is the difference between the positions of the electron at times t and t' from its classical trajectory $\vec{s}(t) = \vec{p}t + \frac{E_0}{\omega_L} \vec{e}_L \cos(\omega_L t) + \vec{s}_0$ with Eq. (12), i.e., the electron is liberated at t' and returns to the parent ion at t where \vec{s}_0 is the initial position close to the parent ion in the origin [12]. This finding suggests to introduce the excursion time $\tau = t - t'$ of the electron in the continuum. The matrix elements of the Hessian [Appendix B] are $\frac{\partial^2 S_j^{(m)}(\vec{p}, t, t - \tau)}{\partial p_i \partial p_j} = \tau \delta_{ij}$ and its determinant is τ^3 . At the stationary points of $S_j^{(m)}(\vec{p}, t, t')$, the canonical momentum satisfies

$$\vec{p}_{\text{st}}(t, \tau) = -\frac{E_0}{\omega_L \tau} \vec{e}_L [\cos(\omega_L t) - \cos(\omega_L (t - \tau))] , \quad (43)$$

and the quasiclassical action (42) [110] is

$$\begin{aligned} S_{\text{st},j}^{(m)}(t, \tau) = & \left(\frac{\lambda_j^{(m)}}{2} + \mathcal{I}_P + U_P \right) \tau \\ & - 2 \frac{U_P}{\omega_L^2 \tau} (1 - \cos(\omega_L \tau)) \\ & - \frac{U_P}{\omega_L} C(\tau) \cos(\omega_L (2t - \tau)) , \end{aligned} \quad (44)$$

with the ponderomotive potential [126, 127] of the optical laser $U_P = \frac{E_0^2}{4\omega_L}$ and

$$C(\tau) = \sin(\omega_L \tau) - \frac{4}{\omega_L \tau} \sin^2\left(\omega_L \frac{\tau}{2}\right) . \quad (45)$$

Equation (43) becomes Eq. (14) in Ref. 12 by dropping the factors \bar{e}_L , ω_L and making the replacement $-E_{0L} \rightarrow E$. I find that Eq. (44) is transformed into Eq. (15) of Ref. 12 by omitting ω_L and replacing $\frac{\lambda_j^{(m)}}{2} + \mathcal{I}_P \rightarrow I_P$. Apart from the extra factors ω_L in Eq. (45), it is the same as Eq. (16) in Ref. 12.

The dipole components (41) for $i \in \{a, c\}$, $j \in \{+, -\}$, and $m \in \mathbb{M}_2$ in saddle-point approximation are simplified as the quadruple integral over the canonical momentum \vec{p} and the time t' is replaced by a single integral over the excursion time τ leading to

$$\begin{aligned} \mathfrak{D}_{ij}^{(m)}(t) &= -i(-1)^{\delta_{ic}} U_{ij}^{(m)} w_j^{(m)} e^{-i\delta_{ic}\omega_X t} a^*(t) \\ &\times \int_0^\infty \sqrt{\frac{(-2\pi i)^3}{\tau^3}} a(t-\tau) \mathfrak{A}_i^{(m)}(t, \tau) \\ &\times e^{-iS_{st,j}^{(m)}(t, \tau)} d\tau, \end{aligned} \quad (46)$$

upon extending the integration over τ to infinity and introducing the field-dipole product with $i \in \{a, c\}$ at the stationary points of the quasiclassical action by

$$\begin{aligned} \mathfrak{A}_i^{(m)}(t, \tau) &= E_L(t-\tau) \varphi_{H, \vec{p}_{st}(t, \tau) + \vec{A}_L(t)}^{(m)*} \\ &\times \varphi_{L, \vec{p}_{st}(t, \tau) + \vec{A}_L(t-\tau)}^{(m)} a. \end{aligned} \quad (47)$$

The factor $\sqrt{\frac{(-2\pi i)^3}{\tau^3}}$ in Eq. (46) stems from the integration over \vec{p} in saddle-point approximation [Appendix B].

The dipole components without x rays $\mathfrak{d}^{(m)}(t)$ for $m \in \mathbb{M}_1$ are obtained from the case $i = a$ and $j = +$ in Eq. (46) by replacing $(-1)^{\delta_{ic}} U_{ij}^{(m)} w_j^{(m)} e^{-i\delta_{ic}\omega_X t} \rightarrow 1$ and $\lambda_\pm^{(m)} \rightarrow -\delta - i\Gamma_a$ in Eq. (44).

The resulting equation becomes the same as Eq. (13) in Ref. 12—by setting $\epsilon = 0$ and suppressing the c.c. summand there—and further replacing $a^*(t) \rightarrow -1$ and $a(t-\tau) \rightarrow 1$. Additionally, Eq. (47) needs to be changed, before it is inserted into Eq. (46), by replacing $E_L(t) \rightarrow E \cos(t-\tau)$, $\varphi_{H, \vec{p}_{st}(t, \tau) + \vec{A}_L(t)}^{(m)*} \rightarrow d_x^*(p_{st}(t, \tau) - A_x(t))$, $\varphi_{L, \vec{p}_{st}(t, \tau) + \vec{A}_L(t-\tau)}^{(m)} \rightarrow d_x(p_{st}(t, \tau) - A_x(t-\tau))$ and adapting $\vec{p}_{st}(t, \tau)$ from Eq. (43) as for Eq. (14) from Ref. 12. Finally, Eq. (44) is adapted as for Eq. (9) in Ref. 12 and I let $m = 0$ in Eq. (46).

The field-dipole product (47) is periodic in time with the optical-laser period $T_L = \frac{2\pi}{\omega_L}$ and can thus be expanded into a Fourier series [12, 123] for $i \in \{a, c\}$ yielding

$$\mathfrak{A}_i^{(m)}(t, \tau) = \sum_{M=-\infty}^{\infty} \tilde{\mathfrak{A}}_{M,i}^{(m)}(\tau) e^{-i(2M+\delta_{ia})\omega_L t}, \quad (48)$$

with the Fourier coefficients

$$\tilde{\mathfrak{A}}_{M,i}^{(m)}(\tau) = \frac{1}{T_L} \int_0^{T_L} \mathfrak{A}_i^{(m)}(t, \tau) e^{i(2M+\delta_{ia})\omega_L t} dt. \quad (49)$$

The $\tilde{\mathfrak{A}}_{M,i}^{(m)}(\tau)$ for $i \in \{a, c\}$ reflect the symmetry properties of the involved atomic states: the Fourier coefficients for M odd (even)—restricted to an integration range from 0 to $T_L/2$ —can be examined by substituting $t \rightarrow t + \frac{T_L}{2}$. Using Eqs. (12), (36), (43), and (47) with this replacement, I find that the kinetic momentum in the argument of the dipole matrix elements in Eq. (47) is negated. To investigate the consequences of the substitution $\vec{k} \rightarrow -\vec{k}$ for the atomic dipole matrix element $\varphi_{j, \vec{k}i}^{(m)}$ for $i \in \{a, c\}$, I express it with Eq. (1) and the spatial atomic orbital $\langle \vec{r} | i; m \rangle$ as follows

$$\varphi_{j, \vec{k}i}^{(m)} = \frac{1}{(2\pi)^{3/2}} \int_{\mathbb{R}^3} e^{-i\vec{k}\cdot\vec{r}} \vec{e}_j \cdot \vec{r} \langle \vec{r} | i; m \rangle d^3r, \quad (50)$$

for $j \in \{L, H\}$. The central symmetry of the atomic potential implies that the orbitals are parity eigenstates [118] and a spatial inversion $\vec{r} \rightarrow -\vec{r}$ yields $\varphi_{j, -\vec{k}i}^{(m)} = \pm \varphi_{j, \vec{k}i}^{(m)}$ depending on the parity of $|i; m\rangle$. Going back to the analysis of Eq. (49), I find that for $i = a$, the even Fourier coefficients vanish. As $a \rightarrow c$ is an electric dipole transition, the one-electron states $|a; m\rangle$ and $|c; m\rangle$ have opposite parity [134]. Therefore, for $i = c$, the odd Fourier coefficients are zero. In Appendix A 2, Eq. (50) is decomposed into a sum over radial integrals times spherical harmonics times Clebsch-Gordan coefficients.

E. High-order harmonic spectrum

1. Harmonic photon emission rate

The HH spectrum for low ground state depopulation due to ionization by the optical laser and the x rays is calculated by setting $\Gamma_0 = 0$. In this case, $a(t) \approx 1$ for all times t and Eq. (19) can be neglected altogether. *Without* the ω_X -dependent term, the dipole components [Eq. (46)] are periodic with period T_L because, in general, ω_X is not a harmonic of ω_L . Consequently, $e^{i\delta_{ic}\omega_X t} \mathfrak{D}_{ij}^{(m)}(t)$ can be expanded into a Fourier series in analogy to Eqs. (48) and (49). The even (odd) Fourier coefficients of $e^{i\delta_{ic}\omega_X t} \mathfrak{D}_{ij}^{(m)}(t)$ are present when the even (odd) Fourier coefficients of the Fourier series expansion of the field-dipole product (48) are nonzero.

I simplify $e^{i\delta_{ic}\omega_X t} \mathfrak{D}_{ij}^{(m)}(t)$ [Eq. (46)] by expanding the exponential of the quasiclassical action by decomposing the t -dependent terms in $e^{-iS_{st,j}^{(m)}(t, \tau)}$ with the Jacobi-Anger expansion

$$e^{iz \cos \theta} = \sum_{M=-\infty}^{\infty} i^M J_M(z) e^{-iM\theta}, \quad (51)$$

involving the Bessel functions $J_M(z)$ [123] by letting $\theta = \omega_L(2t - \tau)$ and $z = \frac{U_P}{\omega_L} C(\tau)$. The expression for the Fourier coefficients of the dipole components (46), with

the dependence on ω_X removed and an extra factor 2π introduced, reads

$$\begin{aligned} \tilde{\mathcal{D}}_{ij,2K+\delta_{i_a}}^{(m)} &= \frac{2\pi}{T_L} \int_0^{T_L} e^{i\delta_{i_c}\omega_X t'} \mathcal{D}_{ij}^{(m)}(t') \\ &\quad \times e^{i(2K+\delta_{i_a})\omega_L t'} dt' \quad (52) \\ &= -2\pi i (-1)^{\delta_{i_c}} U_{ij}^{(m)} w_j^{(m)} \int_0^\infty \sqrt{\frac{(-2\pi i)^3}{\tau^3}} \\ &\quad \times e^{-iF_{0,j}^{(m)}(\tau)} \sum_{M=-\infty}^\infty \tilde{\mathfrak{A}}_{K-M,i}^{(m)}(\tau) i^M \\ &\quad \times J_M\left(\frac{U_P}{\omega_L} C(\tau)\right) e^{iM\omega_L\tau} d\tau, \end{aligned}$$

where the integration over t' leads to δ_{K-MN} , I translate the sum by $M \rightarrow K - M$, and define

$$\begin{aligned} F_{0,j}^{(m)}(\tau) &= \frac{\lambda_j^{(m)}}{2} \tau + F_0'(\tau) \\ &= \left(\frac{\lambda_j^{(m)}}{2} + \mathcal{I}_P + U_P\right) \tau \quad (53) \\ &\quad - 2\frac{U_P}{\omega_L^2} (1 - \cos(\omega_L \tau)). \end{aligned}$$

Inspecting Eqs. (52) and (53), I find that there is a $e^{-i\frac{\lambda_j^{(m)}}{2}\tau}$ dependence of the integrand in Eq. (52). The eigenvalues of the Rabi matrix (31) have a negative imaginary summand $-\frac{i}{2}(\Gamma_a + \Gamma_c)$ which causes $e^{-i\frac{\lambda_j^{(m)}}{2}\tau}$ to acquire an exponentially decaying factor. In other words, the longer the excursion time of an electron in the continuum, the stronger is the suppression of its contribution to the HH spectrum due to destruction of the system by ionization and decay. This reduces the importance of long trajectories versus short trajectories further in addition to the reduction due to the increased spreading of the wave packet (17) for long trajectories in the continuum [11, 12]. Along the same line, multiple returns of the continuum electron to the nucleus are disadvantaged.

The expression for $\tilde{\mathfrak{d}}_{2K+1}^{(m)}$ for $m \in \mathbb{M}_1$ is obtained from the case $i = a$ and $j = +$ in Eq. (52) by letting $\lambda_0^{(0)} = -\delta - i\Gamma_a$ in Eq. (53) and changing $(-1)^{\delta_{i_c}} U_{ij}^{(m)} w_j^{(m)} \rightarrow 1$ and $F_{0,j}^{(m)}(\tau) \rightarrow F_{0,0}^{(m)}(\tau)$.

From the expression for $\tilde{\mathfrak{d}}_{2K+1}^{(m)}$, Eq. (18) of Ref. [12] follows by the replacements $-2\pi i \rightarrow i$, $\tilde{\mathfrak{A}}_{K-M,i}^{(m)}(\tau) \rightarrow b_{K-M}(\tau)$ and $\omega_L \rightarrow 1$ —where the modification $\omega_L \rightarrow 1$ is made to Eq. (48) and $C(\tau)$ is adapted as before—and truncating the $\sum_{M=-\infty}^\infty$ to $\sum_{M=0}^\infty$ and expressing the factor from the saddle-point approximation with the infinitesimal ϵ set to zero. After removing the ω_L from $F_{0,j}^{(m)}(\tau)$,

the replacement $\frac{\lambda_j^{(m)}}{2} + \mathcal{I}_P \rightarrow I_P$ in $F_{0,j}^{(m)}(\tau)$ turns it into $F_0(\tau)$ after Eq. (18) in Ref. 12.

The dipole moment $\mathcal{D}(t)$ [Eq. (40)] is obtained from the Fourier coefficients of the dipole components (52), with the ω_X -dependence removed, as follows:

$$\mathcal{D}(t) = \frac{1}{2\pi} \sum_{\substack{i \in \{a,c\} \\ j \in \{+,-\}}} \sum_{K=-\infty}^\infty \tilde{\mathfrak{D}}_{ij,2K+\delta_{i_a}} e^{-i[(2K+\delta_{i_a})\omega_L + \delta_{i_c}\omega_X]t}, \quad (54)$$

with the compact notation for the dipole components

$$\tilde{\mathfrak{D}}_{ij,2K+\delta_{i_a}} = \frac{\delta_{i_a}}{2} \sum_{m \in \mathbb{M}_1} \tilde{\mathfrak{d}}_{2K+1}^{(m)} + \sum_{m \in \mathbb{M}_2} \tilde{\mathfrak{d}}_{ij,2K+\delta_{i_a}}^{(m)}, \quad (55)$$

where the prefactor $\frac{\delta_{i_a}}{2}$ ensures that only for valence recombination, i.e., $i = a$, the $\tilde{\mathfrak{d}}_{2K+1}^{(m)}$ make a contribution and the sum over j in Eq. (54) removes the prefactor $\frac{1}{2}$. The Fourier coefficients for negative K correspond to the inverse process in which the HH photon is emitted before the required number of optical laser photons is absorbed to satisfy energy conservation [14]. The energies of the emitted HH photons are certainly the same as in the regular process. The inverse process is strongly suppressed because the responsible Fourier coefficients have a highly oscillatory integrand and thus are very small; hence, they may be omitted in Eq. (54) as in Ref. 12. I express $\mathcal{D}(t)$ in frequency domain by a Fourier transformation

$$\begin{aligned} \tilde{\mathcal{D}}(\omega) &= \int_{-\infty}^\infty \mathcal{D}(t) e^{i\omega t} dt \\ &= \sum_{\substack{i \in \{a,c\} \\ j \in \{+,-\}}} \sum_{K=-\infty}^\infty \tilde{\mathfrak{D}}_{ij,2K+\delta_{i_a}} \\ &\quad \times \delta((2K + \delta_{i_a})\omega_L + \delta_{i_c}\omega_X - \omega), \quad (56) \end{aligned}$$

where I use the representation

$$\int_{-\infty}^\infty e^{i\omega t} dt = 2\pi \delta(\omega), \quad (57)$$

of the Dirac δ distribution [123].

The HH spectrum is given by the frequency-resolved and solid-angle-dependent rate of HH photon emission [12, 14, 15] where I consider only HH emission along the x axis with polarization vector $\vec{e}_H = \vec{e}_z$. The derivation in Appendix C 2 leads to

$$\frac{\partial^2 \Gamma_H(\omega)}{\partial \omega \partial \Omega} = 8\pi^2 \omega \varrho(\omega) W(\omega), \quad (58)$$

with the solid angle Ω into which the HH photons are emitted. The density of free-photon states in the photon energy interval $[\omega; \omega + d\omega]$ [92, 93], for a fixed polarization \vec{e}_z and propagation along \vec{e}_x , reads

$$\varrho(\omega) = \frac{\omega^2}{(2\pi)^3 c^3}, \quad (59)$$

with the speed of light c in vacuum, and

$$W(\omega) = W_1(\omega) + \sum_{H=1}^{\infty} \delta_{(2H+1)\omega_L, \omega_X} W_{2,H}(\omega) \quad (60a)$$

$$W_1(\omega) = \sum_{K=-\infty}^{\infty} \sum_{\substack{i \in \{a,c\} \\ j, j' \in \{+, -\}}} [\check{\mathfrak{D}}_{ij, 2K+\delta_{i_a}}^* \check{\mathfrak{D}}_{ij', 2K+\delta_{i_a}}] \times \delta((2K + \delta_{i_a})\omega_L + \delta_{i_c}\omega_X - \omega) \quad (60b)$$

$$W_{2,H}(\omega) = \sum_{K=-\infty}^{\infty} \sum_{j, j' \in \{+, -\}} [\check{\mathfrak{D}}_{aj, 2K+1}^* \check{\mathfrak{D}}_{cj', 2(K-H)} + \text{c.c.}] \times \delta((2K + 1)\omega_L - \omega). \quad (60c)$$

With “c.c.” I denote the complex conjugate of the preceding summand. The HH spectrum consist, via Eq. (56), of discrete lines where the coefficients in front of the Dirac δ distributions represent the strength of the respective HH emission line. The width of the lines, however, is zero, despite the widths of the singly-excited states $|\Phi_{\vec{k}}^{(m_1)}\rangle$, $|\Phi_{\vec{k}_c}^{(m_2)}\rangle$, and $|\Phi_{\vec{k}_a}^{(m_2)}\rangle$ for $m_1 \in \mathbb{M}_1$ and $m_2 \in \mathbb{M}_2$, in Eq. (17) with destruction rates Γ_a and Γ_c , respectively. The widths Γ_a and Γ_c enter Eq. (46) only via $U_{ij}^{(m_2)}$, $w_j^{(m_2)}$, and $\lambda_j^{(m_2)}$ which do not depend on t and thus cause only a change of the strength of the lines.

There are several contributions to the HH rate in Eq. (58) which I analyze in the following. If $\omega_X = (2H + 1)\omega_L$ holds for an $H \in \mathbb{N}$, then I obtain $W(\omega) = W_1(\omega) + W_{2,H}(\omega)$ from Eq. (60). The HH lines due to the recombination with the core hole align with higher orders of the HH emission from the recombination with a valence hole, if the latter plateau is sufficiently extended. Then this leads to interference between the light from both processes mediated by $W_{2,H}(\omega)$. Otherwise, if ω_X is *not* an odd harmonic of ω_L , then Eq. (60) reduces to $W(\omega) = W_1(\omega)$ and the lines in the HH spectrum belong to two distinct groups: first, $i = a$, HH light from the recombination with the valence vacancy gives rise to lines at the energies $(2K + 1)\omega_L$ for $K \in \mathbb{Z}$. The x rays induce interference effects in the recombination step via the two x-ray dressed states with $j \in \{+, -\}$. If the x rays are sufficiently intense, the core electron in the two-level system may even undergo Rabi flopping [71, 75, 88–93, 103–106] prior recombination of the continuum electron. In the bare-states picture, this means that there are multiple pathways for the recombination with the valence hole: once, direct recombination and, alternatively, recombination after an even number of Rabi cycles of the second electron. Second, $i = c$, HH light due to recombination with the x-ray dressed core vacancy leads to lines at energies $2K\omega_L + \omega_X$ for $K \in \mathbb{Z}$. In other words, the energy of the HH photons from a recombination with a core hole are shifted by the photon energy of the x rays ω_X to higher energies. In the bare-states picture, there are multiple pathways: once, recombination with the core hole after excitation of a core electron into the valence

vacancy and, alternatively, recombination after an odd number of Rabi cycles of the second electron.

The HH spectrum (58) gives the emission rate of HH photons into a small solid angle centered on \vec{e}_x with specific energy. However, the experimental observable of HHG is the harmonic photon number spectrum (HPNS) [135]. The HPNS from a single atom is the probability to observe a HH photon in a solid angle Ω with specific energy ω after irradiation of the atom with a light pulse. It is obtained along the x axis from Eq. (58) by multiplying with the pulse duration T_P of the optical laser and the x rays [136] for which the HPNS is recorded. The photon-energy-resolved and solid-angle-resolved HPNS is given by the probability density

$$\frac{\partial^2 P_H(\omega)}{\partial \omega \partial \Omega} = T_P \frac{\partial^2 \Gamma_H(\omega)}{\partial \omega \partial \Omega}. \quad (61)$$

The integration $\int_{\Delta\Omega} \int_{\omega_H - \Delta\omega_H}^{\omega_H + \Delta\omega_H} d\omega d\Omega$ of $\frac{\partial^2 \Gamma_H(\omega)}{\partial \omega \partial \Omega}$ over the solid angle $\Delta\Omega$ and the photon energy range $[\omega_H - \Delta\omega_H; \omega_H + \Delta\omega_H]$ yields the rate for the atom to emit a HH photon per unit of time in the course of the interaction with the light pulses.

In Fig. 35.2 of Ref. 81, we display XUV/x-ray boosted HH spectra for XUV/x-ray light tuned to the $\text{Kr}^+ 3d \rightarrow 4d$ and $\text{Ne}^+ 1s \rightarrow 2p$ transitions in the parent ions. Two plateaux are visible from valence- and core-hole recombinations that are separated by the photon energy of the XUV/x-ray light. The amplitude of the plateaux depends on the intensity of the XUV/x-ray light. By adjusting the intensity suitably, a similar amplitude of both plateaux is achieved.

2. Harmonic photon number spectrum

When the influence on the HH spectrum from ground state depopulation due to ionization by the optical laser and the x rays becomes appreciable, one needs to account for it by letting $\Gamma_0 > 0$. This, however, breaks the periodicity in time imposed by assuming a cw optical laser and cw x rays such that one needs to assume finite optical-laser and x-ray pulses with a constant field strength starting at $t = 0$ and ending at $t = T_P$. In doing so, the x-ray dressed states of Eq. (35) become an approximation for the nonperiodic system.

To determine the time-dependent ground-state amplitude, I need to solve Eq. (19) where I drop the second term on the right-hand side and include its influence—the destruction of the system by tunnel ionization [96–102] via the optical laser—in Γ_0 . For a constant ionization rate $\Gamma_0 > 0$ [Eq. (7)] beginning at $t = 0$ and ending at $t = T_P$, the ground-state amplitude is

$$a(t) = \theta(-t) + e^{-\frac{\Gamma_0}{2}t} \theta(t) \theta(T_P - t) + e^{-\frac{\Gamma_0}{2}T_P} \theta(t - T_P), \quad (62)$$

with the Heaviside step function θ and $\theta(0) = \frac{1}{2}$ [123]. Clearly, $a(t)$ is not periodic in time.

Due to the lack of temporal periodicity of the dipole components—with the ω_X -dependence removed—when $a(t)$ from Eq. (62) is inserted into Eq. (46), the HH spectrum cannot be expanded into a Fourier series any longer, i.e., a HH photon emission rate [compare Eq. (58)] cannot be defined anymore. I need to calculate the Fourier transform of $\mathcal{D}(t)$ [Eq. (40)] instead [12, 14, 15] in order to determine the HPNS [compare Eq. (61)] directly. As a Fourier transform is linear [123], it is applied component-wise. The dipole components (46) in frequency domain for $m \in \mathbb{M}_2$ read

$$\begin{aligned} \tilde{\mathcal{D}}_{ij}^{(m)}(\omega) &= \int_0^{T_P} \mathcal{D}_{ij}^{(m)}(t) e^{i\omega t} dt \\ &= -2\pi i (-1)^{\delta_{i,c}} U_{ij}^{(m)} w_j^{(m)} \int_0^\infty \sqrt{\frac{(-2\pi i)^3}{\tau^3}} \\ &\quad \times e^{-iF_{0,j}^{(m)}(\tau)} \sum_{N=-\infty}^\infty i^N J_N\left(\frac{U_P}{\omega_L} C(\tau)\right) e^{iN\omega_L\tau} \\ &\quad \times \sum_{M=-\infty}^\infty \tilde{\mathcal{A}}_{M-N,i}^{(m)}(\tau) h_{M,i}(\omega, \tau) d\tau, \end{aligned} \quad (63)$$

where I expand the exponential of the quasiclassical action at the stationary point in analogy to the derivation of Eq. (52), translate the sum over M by $M \rightarrow M - N$, and define the HH line shape by

$$\begin{aligned} h_{M,i}(\omega, \tau) &= \frac{1}{2\pi} \int_0^{T_P} e^{-i[(2M+\delta_{i,a})\omega_L + \delta_{i,c}\omega_X - \omega]t} \\ &\quad \times a^*(t) a(t - \tau) dt. \end{aligned} \quad (64)$$

The time integration in Eq. (63) extends only from 0 to T_P as the optical laser and x-ray pulses lie in this time interval. The equation has a straightforward interpretation: comparing it with the result without ground-state depletion (56), I see that the Dirac δ distribution HH line shapes in the latter equation are replaced with finite-width line shapes (64) in the former. Yet Eq. (64) still depends on τ which is integrated over in Eq. (63) in contrast to Eq. (56). Ground-state depletion thus causes a finite width of the HH lines.

Using expression (62) for the ground-state depletion, from Eq. (64), I find the HH line shape [110] to be

$$\begin{aligned} h_{M,i}(\omega, \tau) &\approx \frac{e^{\frac{\Gamma_0}{2}\tau}}{2\pi} \\ &\quad \times \frac{e^{-(\Gamma_0+i(\tilde{\omega}_{M,i}-\omega))\tau} - e^{-(\Gamma_0+i(\tilde{\omega}_{M,i}-\omega))T_P}}{\Gamma_0 + i(\tilde{\omega}_{M,i} - \omega)}. \end{aligned} \quad (65)$$

The absolute value of the denominator of $h_{M,i}(\omega, \tau)$ is minimal at $\omega = \tilde{\omega}_{M,i}$ for

$$\tilde{\omega}_{M,i} = (2M + \delta_{i,a})\omega_L + \delta_{i,c}\omega_X. \quad (66)$$

In other words, the HH peaks with ground-state depletion are centered on the positions of the harmonics without ground-state depletion; for $i = c$, the harmonics are

shifted by ω_X with respect to the harmonics for $i = a$. The Eqs. (63) and (65) depend on the excursion time τ of the electron in the continuum which distributes the electron's contribution to HH emission over all harmonic peaks. Yet the dependence on $\tilde{\omega}_{M,i} - \omega$ ensures that only a sizable contribution is made for the peak around $\tilde{\omega}_{M,i}$ to which the return energy of the continuum electron corresponds. For $T_P \rightarrow \infty$, the $4\pi\Gamma_0 |h_{M,i}(\omega, 0)|^2$ is a Lorentzian of a FWHM of $2\Gamma_0$. In Ref. 80, Eq. (6), the factor 2π was not included in the definition of the HH line shape (65) and integration started at 0 instead of τ .

Next I turn to the dipole components $\tilde{\mathcal{D}}^{(m)}(\omega)$ for $m \in \mathbb{M}_1$. They follow from the case $i = a$ and $j = +$ in Eq. (63) by the replacements $(-1)^{\delta_{i,c}} U_{ij}^{(m)} w_j^{(m)} \rightarrow 1$, and $F_{0,j}^{(m)}(\tau) \rightarrow F_{0,0}^{(0)}(\tau)$. Additionally, $\lambda_0^{(0)} = -\delta - i\Gamma_a$ holds and the HH line shape $h_{M,i}(\omega, \tau)$ is given by Eq. (65).

From the Fourier transform of the dipole components, I calculate the HPNS. For this, I introduce the compact notation [see also Eq. (54)]:

$$\tilde{\mathcal{D}}(\omega) = \sum_{\substack{i \in \{a,c\} \\ j \in \{+,-\}}} \tilde{\mathcal{D}}_{ij}(\omega), \quad (67)$$

with [see also Eq. (55)]

$$\tilde{\mathcal{D}}_{ij}(\omega) = \frac{\delta_{i,a}}{2} \sum_{m \in \mathbb{M}_1} \tilde{\mathcal{D}}^{(m)}(\omega) + \sum_{m \in \mathbb{M}_2} \tilde{\mathcal{D}}_{ij}(\omega). \quad (68)$$

Then the HH photon-energy-resolved and solid-angle-resolved HPNS for a single atom—the probability density of emitting a HH photon with specified energy along the x axis—is derived in Appendix C 3 and is given by

$$\frac{\partial^2 P_H(\omega)}{\partial\omega \partial\Omega} = 4\pi\omega \varrho(\omega) |\tilde{\mathcal{D}}(\omega)|^2, \quad (69)$$

similar to Eq. (58).

An emission rate of HH photons can be obtained from the HPNS (69), if its temporal evolution is known via $\frac{\partial}{\partial t} \frac{\partial^2 P_H'(\omega, t)}{\partial\omega \partial\Omega}$. This instantaneous HH emission rate (not optical-laser-cycle averaged), however, presently cannot be determined experimentally and thus is of little use in contrast to the rate for HH emission without ground-state depletion (58). However, an average HH emission rate for harmonic H can be determined from the HPNS (69) via

$$\frac{\partial^2 \bar{\Gamma}_H(\omega)}{\partial\omega \partial\Omega} = \frac{1}{T_P} \frac{\partial^2 P_H(\omega)}{\partial\omega \partial\Omega}. \quad (70)$$

An integration similar to the one after Eq. (61) may be used to determine the probability for an atom to emit a HH photon in the course of the interaction with the light pulses of duration T_P . Dividing by T_P then gives the average rate of HH photon emission. This is the inverse expression to Eq. (61) where the HPNS is determined from the HH rate. In Sect. V of Ref. 12, an approximation for the average HH emission rate is constructed from $|\tilde{\mathcal{D}}(\tilde{\omega}_{M,i})|^2$ for nonvanishing ground-state

depletion by multiplying its value at the position of a HH peak $\omega = \tilde{\omega}_{M,i}$ with a factor that accounts for the area of the peak.

The Fig. 2 of Ref. 80 shows XUV enhanced HHG for the $\text{Kr}^+ 3d \rightarrow 4d$ transition in the parent ion with ground state depletion and Fig. 35.2 of Ref. 81 shows a comparison between XUV/x-ray boosting with and without ground-state depletion for the transitions $\text{Kr}^+ 3d \rightarrow 4d$ and $\text{Ne}^+ 1s \rightarrow 2p$. Two XUV/x-ray intensities are investigated: for the lower intensity the plateaux due to core-hole recombination have low amplitude whereas for the higher intensity roughly the same amplitude is found for valence- and core-hole recombination. For low XUV/x-ray intensity there is a very good agreement between the HH spectra with treating ground-state depletion and without treating it. This agreement, however, becomes less good for high XUV/x-ray intensity due to increased destruction of the system by XUV/x-ray-based ionization.

3. Cutoff law

The cutoff of the HH spectrum with resonant excitation by x rays is changed dramatically with respect to the optical laser-only case. First, inspecting Eq. (40), I see that the terms for the recombination of the continuum electron with a core hole are shifted by ω_X towards higher energy compared with the terms for the recombination with a valence hole. Second, the phenomenological semiclassical cutoff law of an optical laser-only HH spectrum [9–12] is given by

$$\omega_{\text{cut}} = 3.17 U_P + I_P, \quad (71)$$

with the valence ionization potential of the atom I_P . X-ray dressing leads, however, to a different situation; namely, I observe that Eq. (40) contains two terms with $j \in \{-, +\}$ for valence- and core-hole recombination. Associated with the x-ray-dressed states are the energies $\frac{\lambda_j^{(m)}}{2} + \mathcal{I}_P$ [Eq. (21)]. Consequently, there are two contributions shifted for each recombination spectrum with respect to each other. Inserting them for I_P in Eq. (71), I see that the two terms of valence- and core-hole recombination have different cutoffs due to $\lambda_{\pm}^{(m)}$; the larger of the two terms determines the cutoff of the valence- and core-hole recombination HH spectra.

III. HIGH-ORDER HARMONIC GENERATION WITH ARBITRARILY-SHAPED X-RAY PULSES

The formalism of the previous Sect. II relies on an x-ray-dressed-states picture [Eq. (35)] that is only sensible for constant-amplitude x rays [Eq. (14)]. For arbitrarily-shaped x-ray pulses, this is no longer practicable. In this section, I pursue a derivation of x-ray-boosted HHG that circumvents the x-ray-dressed-states

picture. This generalization is motivated by the fact that highly-intense x rays are presently only available from free electron lasers [63–65] that frequently operate by the SASE principle [66–68] and consequently have short temporal coherence with a rapidly fluctuating pulse envelope. Those expressions in this section which have counterparts in Sect. II are noted with the same symbols but with a prime attached.

A. Hamiltonian and equations of motion

I assume an optical laser which produces pulses of a constant amplitude starting at $t = 0$ and stopping at $t = T_P$. So the optical laser is basically approximated as cw light and the field-dipole product (47) is expanded into a Fourier series. Conversely, the x-ray pulse is chosen to be arbitrarily-shaped inside the time interval $[0; T_P]$ and zero otherwise; it is written as

$$E'_X(t) = \frac{E'_{0X}(t)}{2} [e^{i(\omega_X t + \varphi_X(t))} + e^{-i(\omega_X t + \varphi_X(t))}], \quad (72)$$

where $E'_{0X}(t)$ is the time-dependent amplitude of the pulse and $\varphi_X(t)$ is its time-dependent phase [137]. In order to account for arbitrarily-shaped x-ray pulses in \hat{h}_X [Eq. (14)], I need to replace $E_X(t)$ by $E'_X(t)$ therein. The $N/2$ -electron Hamiltonian for the interaction with the x rays \hat{H}'_X has the same form as Eq. (16) with \hat{h}_X replaced by \hat{h}'_X .

The newly arising time-dependent phase of the x-ray field $\varphi_X(t)$ [Eq. (72)] needs to be taken into account in the ansatz for the $N/2$ -electron wave packet (17); it is modified by multiplying the prefactor of $|\Phi_{ka}^{(m)}\rangle$ by $e^{-i\varphi_X(t)}$ for $m \in \mathbb{M}_2$. With this modified ansatz, I obtain new EOMs which are very similar to the ones obtained previously apart from the phenomenological destruction rates $\Gamma'_0(t)$, $\Gamma'_a(t)$, and $\Gamma'_c(t)$ [Eq. (6)] whose time dependence is now accounted for. Further, I introduce the temporal destruction exponents of the system [82] by the optical laser, the x rays, and decay processes up to time t via

$$F_i(t) = \theta(t) \int_0^t \Gamma'_i(t') dt', \quad (73)$$

for $i \in \{0, a, c\}$. First, the new EOM for the ground-state amplitude is formally identical to Eq. (19). Second, also the new EOMs with $m \in \mathbb{M}_2$ for the amplitude of a continuum electron with a valence hole in the parent ion are formally identical to Eq. (20). So are the valence-only EOMs with $m \in \mathbb{M}_1$. Third, the new EOMs for the amplitude of a continuum electron with a core hole in the parent ion, however, differs from Eq. (23) in the first term on the right hand side that needs to be augmented by the summand $-2\dot{\varphi}_X(t) = -2\frac{d\varphi_X(t)}{dt}$; I use a dot over symbols to denote a time derivative. The new EOMs (20)

and (23) are recast in terms of matrix equations for the combined amplitudes $\vec{b}'^{(m)}(\vec{k}, t) \equiv \begin{pmatrix} b_a'^{(m)}(\vec{k}, t) \\ b_c'^{(m)}(\vec{k}, t) \end{pmatrix}$ [compare with Eq. (27)] which are formally identical to Eq. (29) and read

$$\begin{aligned} \frac{\partial}{\partial t} \vec{b}'^{(m)}(\vec{k}, t) &= -\frac{i}{2} (\mathbf{R}'^{(m)} + (\vec{k}^2 + 2\mathcal{I}_P) \mathbf{1}) \vec{b}'^{(m)}(\vec{k}, t) \\ &+ E_L(t) \frac{\partial}{\partial k_z} \vec{b}'^{(m)}(\vec{k}, t) \\ &- i E_L(t) \wp_{L, \vec{k}a}^{(m)} \begin{pmatrix} 1 \\ 0 \end{pmatrix} a'_0(t), \end{aligned} \quad (74)$$

for $m \in \mathbb{M}_2$ and $\vec{k} \in \mathbb{R}^3$ where the instantaneous Rabi matrix [compare with Eq. (28)] is

$$\begin{aligned} \mathbf{R}'^{(m)}(t) &= -\delta \sigma_z + R_{0X}'^{(m)}(t) \sigma_x \\ &- i \mathbf{diag}(\Gamma_a'(t), \Gamma_c'(t) - 2i\dot{\varphi}_X(t)), \end{aligned} \quad (75)$$

with the Pauli matrices σ_x and σ_z [91, 118].

B. Transformation of the equations of motion

The solution of the EOMs for the one-electron amplitudes with $m \in \mathbb{M}_1$, can be determined, in straight analogy to Sect. II C. In order to solve the system of EOMs [new Eq. (19) and Eqs. (74)], I need to realize that, in contrast to the EOMs for cw x rays, the Rabi matrix $\mathbf{R}'^{(m)}(t)$ [Eq. (75)] is time dependent. Hence a decoupling of the two recombination amplitudes by going to an x-ray dressed-states picture, as in Eq. (33), is no longer possible because the eigenvector matrix of $\mathbf{R}'^{(m)}(t)$ does not commute with the time derivative. However, I can approximately decouple the EOMs [Eq. (74)] as follows. I remove the diagonal elements of $\mathbf{R}'^{(m)}(t)$ for $m \in \mathbb{M}_2$ with the substitution

$$\begin{aligned} b_a'^{(m)}(\vec{k}, t) &= b_a''^{(m)}(\vec{k}, t) e^{\frac{i}{2} \delta t - \frac{F_a(t)}{2}} \\ b_c'^{(m)}(\vec{k}, t) &= b_c''^{(m)}(\vec{k}, t) e^{-\frac{i}{2} \delta t + i\varphi_X(t) - \frac{F_c(t)}{2}}. \end{aligned} \quad (76)$$

I let $\vec{b}''^{(m)}(\vec{k}, t) \equiv \begin{pmatrix} b_a''^{(m)}(\vec{k}, t) \\ b_c''^{(m)}(\vec{k}, t) \end{pmatrix}$ and introduce the temporal destruction exponents from Eq. (73). Inserting the ansatz (76) into Eq. (74) leads to

$$\begin{aligned} \frac{\partial}{\partial t} \vec{b}''^{(m)}(\vec{k}, t) &= \left(-\frac{i}{2} R_{0X}'^{(m)}(t) \Sigma_x(t) \right. \\ &\quad \left. - i \left(\frac{\vec{k}^2}{2} + \mathcal{I}_P \right) \mathbf{1} \right) \vec{b}''^{(m)}(\vec{k}, t) \\ &+ E_L(t) \frac{\partial}{\partial k_z} \vec{b}''^{(m)}(\vec{k}, t) \\ &- i E_L(t) \wp_{L, \vec{k}a}^{(m)} \begin{pmatrix} e^{-\frac{i}{2} \delta t + \frac{F_a(t)}{2}} \\ 0 \end{pmatrix} a'(t), \end{aligned} \quad (77)$$

where I employ the matrix

$$\Sigma_x(t) = \begin{pmatrix} 0 & e^{\Delta(t)} \\ e^{-\Delta(t)} & 0 \end{pmatrix}, \quad (78)$$

with the time- but not momentum-dependent exponent

$$\Delta(t) \equiv -i\delta t + i\varphi_X(t) + \frac{1}{2} (F_a(t) - F_c(t)). \quad (79)$$

A diagonalization of $\Sigma_x(t)$ [Eq. (78)] leads to [110] time-independent eigenvalues

$$\mathbf{\Lambda}' \equiv \mathbf{diag}(\lambda'_+, \lambda'_-) = \sigma_z, \quad (80)$$

and [110] time-dependent eigenvectors

$$\mathbf{U}'(t) = \begin{pmatrix} e^{\Delta(t)} & -e^{\Delta(t)} \\ 1 & 1 \end{pmatrix}. \quad (81)$$

I transform the EOMs (77) to the eigenbasis (81) of $\Sigma_x(t)$ [Eq. (78)]—in analogy to the x-ray-dressed-state basis used before [Eq. (35)]—yielding the new amplitudes [compare with Eq. (33)]:

$$\vec{\mathfrak{b}}'^{(m)}(\vec{k}, t) \equiv \begin{pmatrix} \mathfrak{b}'_+{}^{(m)}(\vec{k}, t) \\ \mathfrak{b}'_-{}^{(m)}(\vec{k}, t) \end{pmatrix} = \mathbf{U}'^{-1}(t) \vec{b}''^{(m)}(\vec{k}, t), \quad (82)$$

and the new EOMs

$$\begin{aligned} \frac{\partial}{\partial t} \vec{\mathfrak{b}}'^{(m)}(\vec{k}, t) &= \left(\dot{\mathbf{U}}'^{-1}(t) \mathbf{U}'(t) - \frac{i}{2} R_{0X}'^{(m)}(t) \mathbf{\Lambda}' \right. \\ &\quad \left. - i \left(\frac{\vec{k}^2}{2} + \mathcal{I}_P \right) \mathbf{1} \right) \vec{\mathfrak{b}}'^{(m)}(\vec{k}, t) \\ &+ E_L(t) \frac{\partial}{\partial k_z} \vec{\mathfrak{b}}'^{(m)}(\vec{k}, t) \\ &- i E_L(t) \wp_{L, \vec{k}a}^{(m)} \vec{w}'(t) a'(t). \end{aligned} \quad (83)$$

I added $\dot{\mathbf{U}}'^{-1}(t) \mathbf{U}'(t) \vec{\mathfrak{b}}'(\vec{k}, t)$ on both sides of Eq. (83) which is the transformation rest that reads using Eq. (79):

$$\dot{\mathbf{U}}'^{-1}(t) \mathbf{U}'(t) = \frac{\dot{\Delta}(t)}{2} (-\mathbf{1} + \sigma_x). \quad (84)$$

The valence ionization fraction in the eigenbasis (81) becomes

$$\begin{aligned} \vec{w}'(t) &\equiv \begin{pmatrix} w'_+(t) \\ w'_-(t) \end{pmatrix} = \mathbf{U}'^{-1}(t) \begin{pmatrix} e^{-\frac{i}{2} \delta t + \frac{F_a(t)}{2}} \\ 0 \end{pmatrix} \\ &= \frac{1}{2} e^{\frac{i}{2} \delta t - i\varphi_X(t) + \frac{F_c(t)}{2}} \begin{pmatrix} 1 \\ -1 \end{pmatrix}, \end{aligned} \quad (85)$$

[compare with Eq. (34)].

C. Iterative solution of the equations of motion

Due to the fact that $\dot{\mathbf{U}}'^{-1}(t) \mathbf{U}'(t)$ [Eq. (84)] is not diagonal and time dependent, I cannot simplify the EOMs further without making additional approximations. Therefore, I derive an iterative solution of the EOMs in what follows.

1. Zeroth-iteration amplitudes

In order to decouple the two differential equations (83), I need to approximate the transformation rest (84) by its diagonal elements, i.e., $\dot{\mathbf{U}}'^{-1}(t) \mathbf{U}'(t) \approx -\frac{\dot{\Delta}(t)}{2} \mathbb{1}$. I refer to this as zeroth iteration and attach a superscript “ $(m,0)$ ” to the involved coefficients.

As in Eq. (37), I make the substitution $\vec{k}' = \vec{k} - \vec{A}_L(t) + \vec{A}_L(t')$ at time t' giving

$$\begin{aligned} \frac{d}{dt'} \vec{\mathbf{b}}'^{(m,0)}(\vec{k}', t') &= -\frac{i}{2} [R'_{0X}(m)(t) \mathbf{\Lambda}' + 2(\mathcal{I}_P - i\dot{\Delta}(t)) \mathbb{1} \\ &\quad + (\vec{k} - \vec{A}_L(t) + \vec{A}_L(t'))^2 \mathbb{1}] \\ &\quad \times \vec{\mathbf{b}}'^{(m,0)}(\vec{k}', t') \\ &\quad - i E_L(t') \wp_{L, \vec{k} - \vec{A}_L(t) + \vec{A}_L(t')}^{(m)} a \\ &\quad \times \vec{w}'^{(m)} a'(t'). \end{aligned} \quad (86)$$

This equation can be integrated exactly [123], analogously to Eq. (38), yielding

$$\begin{aligned} \mathbf{b}'_{\pm}(m,0)(\vec{k}, t) &= -i \int_0^t E_L(t') \wp_{L, \vec{k} - \vec{A}_L(t) + \vec{A}_L(t')}^{(m)} \\ &\quad \times e^{-i S'_{\pm}(m)(\vec{k} - \vec{A}_L(t), t, t')} w'_{\pm}(t') a'(t') dt'. \end{aligned} \quad (87)$$

The quasiclassical action [compare with Eq. (42)]—after introducing the canonical momentum $\vec{p} = \vec{k} - \vec{A}_L(t)$ —is given by

$$\begin{aligned} S'_j(m)(\vec{p}, t, t') &= \frac{1}{2} \int_{t'}^t (\vec{p} + \vec{A}_L(t''))^2 dt'' \\ &\quad + \frac{\lambda'_j}{2} (\Theta^{(m)}(t) - \Theta^{(m)}(t')) \\ &\quad - \frac{i}{2} (\Delta(t) - \Delta(t')) + \mathcal{I}_P(t - t'), \end{aligned} \quad (88)$$

where the area [71, 93] of the x-ray pulse is

$$\Theta^{(m)}(t) = \theta(t) \int_0^t R'_{0X}(m)(t') dt'. \quad (89)$$

2. First-iteration amplitudes

I obtain the zeroth-iteration solution (87) of the coupled EOMs [Eq. (74)] by taking only the diagonal elements of the transformation rest (84) into account. The first-iteration amplitudes $\vec{\mathbf{b}}'^{(m,1)}(\vec{k}, t)$ for $m \in \mathbb{M}_2$ are found by inserting the zeroth-iteration result from Sect. III C 1 into Eq. (83) to specify the off-diagonal elements of Eq. (84). I find with Eqs. (83), (84), and (87)

the first-iteration EOMs

$$\begin{aligned} \frac{\partial}{\partial t} \vec{\mathbf{b}}'^{(m,1)}(\vec{k}, t) &= \left[-i \left(\frac{\vec{k}^2}{2} + \mathcal{I}_P - \frac{i}{2} \dot{\Delta}(t) \right) \mathbb{1} \right. \\ &\quad \left. - \frac{i}{2} R'_{0X}(m)(t) \mathbf{\Lambda}' \right] \vec{\mathbf{b}}'^{(m,1)}(\vec{k}, t) \\ &\quad + E_L(t) \frac{\partial}{\partial k_z} \vec{\mathbf{b}}'^{(m,1)}(\vec{k}, t) \\ &\quad - i E_L(t) \wp_{L, \vec{k} a} \vec{w}'(t) a'(t) \\ &\quad + \frac{1}{2} \dot{\Delta}(t) \sigma_x \vec{\mathbf{b}}'^{(m,0)}(\vec{k}, t). \end{aligned} \quad (90)$$

These equations are still decoupled and can be solved along the lines leading to Eq. (87). By identifying the zeroth-iteration solution (87), I obtain

$$\begin{aligned} \mathbf{b}'_{\pm}(m,1)(\vec{k}, t) &= \mathbf{b}'_{\pm}(m,0)(\vec{k}, t) + \frac{1}{2} \int_0^t \dot{\Delta}(t') \\ &\quad \times e^{-i S'_{\pm}(m)(\vec{k} - \vec{A}_L(t), t, t')} \mathbf{b}'_{\mp}(m,0)(\vec{k}', t') dt' \\ &= \mathbf{b}'_{\pm}(m,0)(\vec{k}, t) + \Delta \mathbf{b}'_{\pm}(m,1)(\vec{k}, t). \end{aligned} \quad (91)$$

D. Electric dipole transition matrix element and high-order harmonic spectrum

The time-dependent $N/2$ -electron dipole transition matrix element follows from Eqs. (39) and (40) to

$$\begin{aligned} \mathcal{D}'(t) &= \langle \Psi'_0, t | \hat{D} | \Psi'_c, t \rangle \\ &= \sum_{m \in \mathbb{M}_1} \mathfrak{d}'^{(m)}(t) + \sum_{\substack{i \in \{a, c\} \\ j \in \{+, -\}}} \sum_{m \in \mathbb{M}_2} \mathfrak{D}'_{ij}(m)(t), \end{aligned} \quad (92)$$

where I denote by $|\Psi'_0, t\rangle$ the ground-state part of the new wave packet (17) and by $|\Psi'_c, t\rangle$ its continuum part [14]. The dipole components $\mathfrak{D}'_{ij}(m)(t)$ for $m \in \mathbb{M}_2$ are found by transforming $\vec{\mathbf{b}}'^{(m)}(\vec{k}, t)$ [Eq. (87)] back to the bare-state amplitudes $\vec{b}'^{(m)}(\vec{k}, t)$ with the inverse of Eqs. (76) and (82); they read for $i \in \{a; c\}$ and $j \in \{-; +\}$:

$$\begin{aligned} \mathfrak{D}'_{ij}(m)(t) &= (-1)^{\delta_{ic}} U'_{ij}(t) e^{i\phi_i(t)} a'^*(t) \\ &\quad \times \int_{\mathbb{R}^3} \wp_{H, i\vec{k}}^{(m)} \mathbf{b}'_j(m)(\vec{k}, t) d^3k, \end{aligned} \quad (93)$$

with the time-dependent phase

$$\phi_i(t) = (-1)^{\delta_{ic}} \frac{\delta}{2} t - \delta_{ic} \omega_X t + i \frac{F_i(t)}{2}. \quad (94)$$

The zeroth-iteration dipole components $\mathfrak{D}'_{ij}(m,0)(t)$ follow immediately by substituting $\mathbf{b}'_j(m,0)(\vec{k}, t)$ [Eq. (87)] for $\mathbf{b}'_j(m)(\vec{k}, t)$ in Eq. (93). Inserting the first-iteration solution (91) into Eq. (93), I arrive at the expansion

$$\mathfrak{D}'_{ij}(m,1)(t) = \mathfrak{D}'_{ij}(m,0)(t) + \Delta \mathfrak{D}'_{ij}(m,1)(t), \quad (95)$$

for the first-iteration dipole components.

1. Zeroth-iteration dipole components

In zeroth-iteration, the dipole components $\mathfrak{D}'_{ij}(m,0)(t)$ [Eq. (93)] are obtained from the zeroth-iteration amplitudes (87). I assume a constant-amplitude optical laser pulse which starts at $t = 0$ and ends at $t = T_P$. As the dipole components (93) are not periodic in time, they are Fourier transformed [12, 14, 15]. I introduce the canonical momentum $\vec{p} = \vec{k} - \vec{A}_L(t)$ and the excursion time $\tau = t - t'$, expand the field-dipole product into a Fourier series [Eqs. (47), (48), (49), and (50)] and make the saddle-point approximation [see Eq. (46) and Appendix B] which yields

$$\begin{aligned} \tilde{\mathfrak{D}}'_{ij}(m,0)(\omega) &= -2\pi (-1)^{\delta_{ic}} i \int_0^\infty \sqrt{\frac{(-2\pi i)^3}{\tau^3}} e^{-iF'_0(\tau)} \\ &\times \sum_{N=-\infty}^{\infty} i^N J_N\left(\frac{U_P}{\omega_L} C(\tau)\right) e^{iN\omega_L\tau} \quad (96) \\ &\times \sum_{M=-\infty}^{\infty} \tilde{\mathfrak{A}}'_{M-N,i}(m)(\tau) h'_{M,i,j}(m,0)(\omega, \tau) d\tau, \end{aligned}$$

where I expand the exponential of the quasiclassical action at the stationary point, use $F'_0(\tau)$ from Eq. (53), $C(\tau)$ from Eq. (45), translate the sum over M by $M \rightarrow M - N$, and define the zeroth-iteration HH line shape [compare with Eq. (64)]:

$$\begin{aligned} h'_{M,i,j}(m,0)(\omega, \tau) &= \frac{1}{2\pi} \int_0^{T_P} e^{-i[(2M+\delta_{ia})\omega_L - \omega]t} e^{i\phi_i(t)} \\ &\times e^{-\frac{i}{2}\lambda'_j(\Theta^{(m)}(t) - \Theta^{(m)}(t-\tau))} \quad (97) \\ &\times e^{-\frac{1}{2}(\Delta(t) - \Delta(t-\tau))} U'_{ij}(t) \\ &\times \omega'_j(t-\tau) a'^*(t) a'(t-\tau) dt. \end{aligned}$$

The result [Eqs. (96) and (97)] has a close resemblance to the dipole components for a constant-amplitude x-ray pulse with ground-state depletion [Eqs. (63) and (64)]. However, here, the eigenvectors $\mathbf{U}'(t)$ transform from a different basis to bare states and are time dependent. Hence $\mathbf{U}'(t)$ and $\vec{w}'(t)$ enter Eq. (97) in contrast to Eq. (64).

To derive a closed-form expression from Eq. (97), I need to solve the new Eq. (19) where I omit the second term on the right-hand side of the equation and account for its influence in $\Gamma'_0(t)$. For an arbitrarily-shaped x-ray pulse and a constant-amplitude optical laser pulse, where both pulses begin at $t = 0$ and end at $t = T_P$, the solution for the ground-state amplitude reads

$$a'(t) = \theta(-t) + e^{-\frac{F_0(t)}{2}} \theta(t) \theta(T_P - t) + e^{-\frac{F_0(T_P)}{2}} \theta(t - T_P), \quad (98)$$

similarly to Eq. (62), however, with Γ_0 replaced by $F_0(t)$. This expression is inserted into Eq. (97) to obtain the line

shape for $m \in \mathbb{M}_2$; I find with Eqs. (80), (81), (85), (89), and (94) the zeroth-iteration HH line shape

$$\begin{aligned} h'_{M,i,j}(m,0)(\omega, \tau) &\approx \frac{(-1)^{\delta_{ic}\delta_{jc}}}{4\pi} \int_0^{T_P} e^{-\frac{F_0(t)+F_0(t-\tau)}{2}} \\ &\times e^{-i[(2M+\delta_{ia})\omega_L + \delta_{ic}\omega_X - \omega]t} \\ &\times e^{\frac{i}{2}(\varphi_X(t) - \varphi_X(t-\tau))} e^{-i\delta_{ic}\varphi_X(t)} \quad (99) \\ &\times e^{-\frac{F_a(t)-F_c(t)+F_a(t-\tau)+F_c(t-\tau)}{4}} \\ &\times e^{-\frac{i}{2}\lambda'_j(\Theta^{(m)}(t) - \Theta^{(m)}(t-\tau))} dt. \end{aligned}$$

Disregarding the impact of the other factors in the equation, the line shape peaks around $\omega = \tilde{\omega}_{M,i}$ [Eq. (66)]. The other factors differ substantially from the result (65). The reason for these contributions to occur is the only partial diagonalization of the instantaneous Rabi matrix (75). High-order harmonic emission is suppressed by the destruction of the ground-state amplitude at the time of tunnel ionization $F_0(t-\tau)$ and at the time of recombination $F_0(t)$. Further, the line-shape depends on $F_a(t)$ and $F_c(t)$ which account for the destruction of the intermediate hole states by the optical laser, the x rays, and decay processes. Inspecting Eq. (31), I see that via Eq. (73) this term and the term depending on the pulse area (89) can be understood to result from $\int_{t-\tau}^t \frac{\lambda_{\pm}^{(m)}}{2} dt$ where I retain only the leading order in the expansion of the complex Rabi frequency $\mu^{(m)} \approx R_{0X}^{(m)}$ in $\lambda_{\pm}^{(m)}$ where $R_{0X}^{(m)}$ is assumed to be large with respect to all other parameters in $\mu^{(m)}$.

The dipole components $\mathfrak{D}'^{(m)}(t)$ for $m \in \mathbb{M}_1$ follow directly as in Sect. IID where I, however, set $\lambda_0'^{(0)} = -\delta$ and the HH line shape is

$$\begin{aligned} h'_M(\omega, \tau) &= \frac{1}{2\pi} \int_0^{T_P} e^{-i[(2M+1)\omega_L - \omega]t} \\ &\times e^{-\frac{F_a(t)-F_a(t-\tau)}{2}} a'^*(t) a'(t-\tau) dt \quad (100) \\ &\approx \frac{1}{2\pi} \int_0^{T_P} e^{-i[(2M+1)\omega_L - \omega]t} \\ &\times e^{-\frac{F_0(t)+F_0(t-\tau)}{2}} e^{-\frac{F_a(t)-F_a(t-\tau)}{2}} dt \end{aligned}$$

Finally, the spectral and solid-angle-dependent probability density of HH emission along the x axis follows in zeroth iteration from Eq. (69).

2. First-iteration dipole components

To obtain first-iteration dipole components, the zeroth-iteration solution [Eq. (87)] is inserted into the expression for $\Delta \mathfrak{b}'_{\pm}(m,1)(\vec{k}, t)$ [Eq. (91)], the two quasiclassical actions

are united and treated with the saddle-point method [Appendix B]. Defining two excursion times $\tau' = t - t'$ and $\tau'' = t - t''$ leads, with the expansion of the field-dipole product (48), to the first-iteration correction of the dipole components (93) that manifests in a first-iteration correction of the HH line shape (97) in Eq. (96); the expression for the first-iteration dipole component corrections $\Delta\tilde{\mathcal{D}}'_{ij}(m,1)(\omega)$ [Eq. (95)] are formally the same as in Eq. (96) when letting $\tau = \tau' + \tau''$, using the identity $\int_0^t d\tau' \int_0^{t-\tau'} d\tau'' = \int_0^t d\tau' \int_{\tau'}^t d\tau = \int_0^t d\tau \int_0^\tau d\tau'$, and extending the upper bound of the outermost integral to $+\infty$. The first-iteration correction to the HH line shape for $m \in \mathbb{M}_2$ is

$$\begin{aligned} \Delta h'_{M,i,j}(m,1)(\omega, \tau) &= \frac{1}{2\pi} \int_0^{T_P} e^{-i[(2M+\delta_{ia})\omega_L - \omega]t} e^{i\phi_i(t)} \\ &\times e^{-\frac{i}{2}\lambda'_j[\Theta^{(m)}(t) + \Theta^{(m)}(t-\tau)]} \\ &\times e^{-\frac{i}{2}(\Delta(t) - \Delta(t-\tau))U'_{ij}(t)} \quad (101) \\ &\times w'_{-j}(t-\tau) a'^*(t) a'(t-\tau) \\ &\times \int_0^\tau \frac{1}{2} \dot{\Delta}(t-\tau') e^{i\lambda'_j\Theta^{(m)}(t-\tau')} d\tau' dt. \end{aligned}$$

The first-iteration correction (101) differs somewhat from the zeroth-iteration expression (97). All factors for the integration over t are the same here as there apart from $w'_{-j}(t-\tau)$ here and $w'_j(t-\tau)$ there. The dependence on $\dot{\Delta}(t-\tau')$ [Eq. (79)] accounts for the off-diagonal matrix elements in Eq. (84); the integral over τ' represents the accumulated influence of the off-diagonal elements at time τ . This integral is not present in Eq. (97).

I obtain a closed-form expression for $\Delta h'_{M,i,j}(m,1)(\omega, \tau)$ from Eq. (101) by inserting Eqs. (80), (81), (85), (89), (94), and (98) which yields

$$\begin{aligned} \Delta h'_{M,i,j}(m,1)(\omega, \tau) &\approx \frac{(-1)^{\delta_{ic}\delta_j-+1}}{4\pi} \int_\tau^{T_P} e^{-\frac{F_0(t)+F_0(t-\tau)}{2}} \\ &\times e^{-i[(2M+\delta_{ia})\omega_L + \delta_{ic}\omega_X - \omega]t} \\ &\times e^{-\frac{i}{2}\varphi_X(t-\tau) + \frac{i}{2}(-1)^{\delta_{ic}}\varphi_X(t)} \\ &\times e^{-\frac{-F_a(t) - F_c(t) + F_a(t-\tau) + F_c(t-\tau)}{4}} \\ &\times e^{-\frac{i}{2}\lambda'_j[\Theta^{(m)}(t) - \Theta^{(m)}(t-\tau)]} \\ &\times \int_0^\tau \frac{1}{2} [-i\delta + i\dot{\varphi}_X(t-\tau')] \quad (102) \\ &\quad + \frac{1}{2} (\Gamma'_a(t-\tau') - \Gamma'_c(t-\tau')) \\ &\quad \times e^{i\lambda'_j\Theta^{(m)}(t-\tau')} d\tau' dt. \end{aligned}$$

The first-iteration HH line shape for $m \in \mathbb{M}_2$ reads

$$h'_{M,i,j}(m,1)(\omega, \tau) = h'_{M,i,j}(m,0)(\omega, \tau) + \Delta h'_{M,i,j}(m,1)(\omega, \tau). \quad (103)$$

The probability of the HH emission along the x axis follows by inserting the sum of the zeroth-iteration dipole components [Eq. (96)] and first-iteration dipole corrections $\Delta\tilde{\mathcal{D}}'_{ij}(m,1)(\omega)$ into Eqs. (68) and (69).

IV. CONCLUSION

I discuss theoretically the impact of x-ray excitation on HHG. For this purpose, I develop a two-electron model that is based on the approach of Lewenstein *et al.* [12] for optical-laser-only HHG. In my model, the first electron from the atomic valence is tunnel ionized and, thereafter, propagates freely in the continuum; a second electron from the atomic core is driven by intense x rays that are tuned to the core-valence resonance in the transient ion. For ultrahigh x-ray intensities, this electron may even Rabi flop between the valence and the core state prior recombination of the continuum electron with the parent ion. The optical laser eventually reverses its direction and the first electron may be driven back to the parent ion where it sees a superposition of valence-hole and core-hole states and recombines with it emitting HH radiation that is characteristic of this superposition. Valence-hole recombination leads to the formation of a first HH plateau which is, apart from a slight influence due to x-ray dressing, the same as the HH plateau that is obtained from optical-laser-only HHG. Core-hole recombination causes the formation of a second HH plateau that is shifted by the x-ray photon energy to larger HH energies with respect to the first plateau. The expressions in this article are formulated for, first, cw optical laser and cw x rays, second, constant-amplitude optical-laser and x rays with finite pulse durations, and, third, a constant-amplitude optical laser together with arbitrarily-shaped x-ray pulses. Yet, for pulsed optical light, one will need to take into account that the field-dipole product (47) can no longer be expanded into a Fourier series (48) and the equations discussed here need to be generalized accordingly. A benefit of the chosen approach here is that the equations can be treated to a large degree analytically in contrast to the case when also the optical laser produces arbitrarily-shaped pulses.

I focus on the HH spectrum of a single atom. However, in experiments, a macroscopic sample is used for HHG. The copropagation of the optical laser together with the x-ray radiation from a FEL and HHG through the gas transforms the HH spectrum significantly due to interference effects caused by coherent emission of light in the sample [18–22]. The phase matching shall be examined in future studies specifically under the objective of the impact of SASE FEL x rays on the HHG process; a simple estimate of the yield of a different x-ray-boostered HHG scheme in SAE—for which tunnel ionization is replaced by one-x-ray-photon ionization of a core electron—shows that a considerable output can be achieved from a macroscopic sample [82].

The model of Lewenstein *et al.* [12] describes excel-

lently qualitatively HH spectra but tends to overestimate the HH yield significantly by roughly two orders of magnitude [138]. The inaccuracies of the model can be mitigated by using the Eikonal-Volkov approximation (EVA) [139] and considering electron correlations [28, 49]. In the case of a SAE, a numerical integration of the time-dependent Schrödinger equation is a route to obtain an accurate HH yield. However, in my case, a numerical integration of a $N/2$ -electron Schrödinger equation would be required with substantially increased complexity [17].

My prediction of x-ray-boostered-HHG offers novel prospects for nonlinear x-ray physics that complements the nonlinear x-ray-only processes of sequential and simultaneous absorption of multiple x rays [140, 141]. Namely, the excursion of the tunnel-ionized electron in the HHG process determines a time window in which resonant x-ray interactions may occur. Rabi flopping is a highly nonlinear fundamental process and becomes experimentally feasible with x rays for the first time using FELs [71, 75, 103–106]. The occurrence of Rabi oscillations of the second electron between valence and core states prior to recombination of the first electron may have a much clearer signature if combined with the HHG scheme compared with the case if only x rays are considered. The manipulation of HHG with x rays may also facilitate frequency-resolved optical gating (FROG) [142, 143] with x-ray pulses thus offering the long-sought after pulse characterization for chaotic SASE FEL x rays [144, 145] but this issue requires further theoretical research. The novel scheme also makes single attosecond x-ray pulses [146, 147] and attosecond x-ray pulse trains [35] feasible using the same methods that are used with conventional HHG which has been predicted recently using one-x-ray-photon ionization of core electrons for boosting HHG [82]. Above all, tomographic imaging of core orbitals with HHG comes into reach [24–28]. Finally, HHG has been used to generate frequency combs in the XUV; potentially, such HHG spectra can be boosted by x rays in order to extend frequency-comb-based spectroscopy to the x-ray regime [148, 149] provided that one has identically-shaped x-ray pulses which are carefully synchronized to the optical laser. This would complement a competing approach of x-ray frequency comb generation using resonance fluorescence and coherent x-ray pulse shaping [75, 150, 151].

ACKNOWLEDGMENTS

I am indebted to Christoph H. Keitel and Markus C. Kohler, for their continuous encouragement, helpful discussions, and a critical reading of the manuscript. I am grateful to Karen Z. Hatsagortsyan, Feng He (何峰), and Robin Santra for helpful discussions. I was supported by a Marie Curie International Reintegration

Grant within the 7th European Community Framework Program (call identifier: FP7-PEOPLE-2010-RG, proposal No. 266551).

Appendix A: Electronic structure

In the nonrelativistic Hartree-Fock-Slater independent-electron approximation [114–117], the electronic structure of an atom is given by the orbital energies [in \hat{h}_A , Eq. (9)] and the spatial atomic orbitals in spherical polar coordinates [123]—with radius $r = ||\vec{r}'||$ and solid angle Ω —expressed by $\langle \vec{r}' | i; m_i \rangle = R_{n_i l_i}(r) Y_{l_i m_i}(\Omega)$ with the radial part $R_{n_i l_i}(r)$ and the angular part, a spherical harmonic [134], $Y_{l_i m_i}(\Omega)$ for $i \in \{a, c\}$ [117]. In optical-laser and x-ray light (8), the spatial orbitals enter the electric dipole transition matrix elements in \hat{h}_L [Eq. (11)], \hat{h}_X [Eq. (14)], and \hat{D} [Eq. (40)]. There are three types of dipole transition matrix elements: first, bound-bound transitions [Sect. A 1] between core and valence states (26), second, bound-continuum transitions [Sect. A 2] between the valence and continuum states (24), and, third, continuum-continuum transitions [Sect. A 3] between continuum states (25).

To express the electric dipole transition operator in terms of spherical polar coordinates [123], I employ the relation

$$\vec{e}_\lambda \cdot \vec{r} = r \sqrt{\frac{4\pi}{3}} Y_{1\lambda}(\Omega), \quad (\text{A1})$$

with $\lambda \in \{-1, 0, 1\}$, $\vec{e}_0 = \vec{e}_z$, and $\vec{e}_{\pm 1} = \mp \frac{1}{\sqrt{2}} (\vec{e}_x \pm i \vec{e}_y)$ [71, 134]. The \vec{e}_{+1} is almost the left-circularly polarization (positive helicity) vector $\vec{e}^{(L)} = -\vec{e}_{+1}$ whereas \vec{e}_{-1} is equal to the right-circularly polarization (negative helicity) vector $\vec{e}^{(R)} = \vec{e}_{-1}$ [152]. In the scalar product $\vec{e}_\lambda \cdot \vec{r}$, complex conjugation is on the second factor, here \vec{r} , which is real throughout.

1. Bound-bound transitions

Electric dipole transition matrix elements between two bound states are expressed in terms of spatial orbitals as in Eq. (50); they are

$$\begin{aligned} \langle c; m_c | \vec{e}_\lambda \cdot \vec{r} | a; m_a \rangle &= \int_{\mathbb{R}^3} \langle c; m_c | \vec{r} \rangle \vec{e}_\lambda \cdot \vec{r} \langle \vec{r} | a; m_a \rangle d^3r \quad (\text{A2}) \\ &= \delta_{m_a \pm \lambda m_c} \sqrt{\frac{4\pi}{3}} \mathcal{Y}(l_a, 1, l_c; m_a, \lambda, m_c) \mathcal{R}_{\text{BB}, ca}, \end{aligned}$$

upon inserting Eq. (A1) and the spatial orbitals $\langle \vec{r}' | i; m_i \rangle = R_{n_i l_i}(r) Y_{l_i m_i}(\Omega)$ with $i \in \{a, c\}$. The angular integral is

$$\begin{aligned} \mathcal{Y}(l_1, l_2, l_3; m_1, m_2, m_3) &= \int_{4\pi} Y_{l_3 m_3}^*(\Omega) Y_{l_2 m_2}(\Omega) Y_{l_1 m_1}(\Omega) d\Omega \\ &= \sqrt{\frac{(2l_1+1)(2l_2+1)}{4\pi(2l_3+1)}} C(l_1, l_2, l_3; m_1, m_2, m_3) C(l_1, l_2, l_3; 0, 0, 0), \end{aligned} \quad (\text{A3})$$

where $C(l_1, l_2, l_3; m_1, m_2, m_3)$ is a Clebsch-Gordan coefficient [134]. The integral restricts the accessible angular momenta and magnetic quantum numbers in the photoexcitation process such that only transitions occur where $m_c = m_a \pm \lambda$ holds for the magnetic and $l_c \in \{|l_a - 1|, l_a + 1\}$ for the angular quantum numbers. The radial dipole matrix element is

$$\mathcal{R}_{\text{BB},ca} = \int_0^\infty R_{n_c l_c}(r) r^3 R_{n_a l_a}(r) dr, \quad (\text{A4})$$

For $\vec{e}_X = \vec{e}_z = \vec{e}_0$, the matrix element in Eq. (26) is obtained from Eq. (A2).

$$\langle \vec{k} | \vec{e}_\lambda \cdot \vec{r} | a; m_a \rangle = 2\sqrt{\frac{2}{3}} \sum_{l \in \{|l_a-1|, l_a+1\}} (-i)^l \mathcal{Y}(l_a, 1, l; m_a, \lambda, m_a + \lambda) Y_{l m_a + \lambda}(\Omega_k) \mathcal{R}_{\text{BC},a}^{(l)}(k). \quad (\text{A7})$$

The radial dipole matrix element is

$$\mathcal{R}_{\text{BC},a}^{(l)}(k) = \int_0^\infty j_l(kr) r^3 R_{n_a l_a}(r) dr. \quad (\text{A8})$$

From expression (A7), I realize that the bound-continuum matrix elements for circularly polarized light, i.e., for $\lambda = \pm 1$, are nonzero [110]. This implies that emission of circularly polarized HH photons may occur also. This is an artifact of choosing plane waves (1) as a basis for continuum electrons instead of the part of them with the appropriate magnetic quantum number m_a . Letting $\vec{e}_H = \vec{e}_z = \vec{e}_0$, as it is done in this article in Eqs. (24) and (40), resolves this issue because then only the correct part with m_a of the plane waves is projected onto.

2. Bound-continuum transitions

Electric dipole transition matrix elements between bound and continuum states [118, 127] read

$$\langle \vec{k} | \vec{e}_\lambda \cdot \vec{r} | a; m_a \rangle = \frac{1}{(2\pi)^{3/2}} \int_{\mathbb{R}^3} e^{-i\vec{k}\cdot\vec{r}} \vec{e}_\lambda \cdot \vec{r} \langle \vec{r} | a; m_a \rangle d^3r. \quad (\text{A5})$$

I use Eq. (A1), the spatial atomic valence orbital $\langle \vec{r} | a; m_a \rangle = R_{n_a l_a}(r) Y_{l_a m_a}(\Omega_r)$, and the spatial part of the plane wave (1). Expression (A5) is recast employing the Rayleigh expansion [134] of plane waves

$$e^{i\vec{k}\cdot\vec{r}} = 4\pi \sum_{l=0}^\infty \sum_{m=-l}^l i^l Y_{l m}^*(\Omega_k) j_l(kr) Y_{l m}(\Omega_r). \quad (\text{A6})$$

The directions of \vec{k} and \vec{r} are specified by the solid angles Ω_k and Ω_r , respectively, and the magnitudes by $k = \|\vec{k}\|$ and $r = \|\vec{r}\|$. Here, j_l denotes a spherical Bessel function [123]. Upon inserting Eq. (A1) into Eq. (A5), I arrive at the dipole matrix element (A5) in spherical polar coordinates,

3. Continuum-continuum transitions

Electric dipole transition matrix elements between two continuum states (1) are given by

$$\begin{aligned} \langle \vec{k} | \vec{e}_\lambda \cdot \vec{r} | \vec{k}' \rangle &= \frac{1}{(2\pi)^{3/2}} \vec{e}_\lambda \cdot \int_{\mathbb{R}^3} e^{-i\vec{k}\cdot\vec{r}} \vec{r} e^{i\vec{k}'\cdot\vec{r}} d^3r \quad (\text{A9}) \\ &= \frac{1}{(2\pi)^{3/2}} \vec{e}_\lambda \cdot \int_{\mathbb{R}^3} (-i) \vec{\nabla}_{\vec{k}'} e^{i(\vec{k}'-\vec{k})\cdot\vec{r}} d^3r. \end{aligned}$$

Using the representation (57) of the Dirac δ distribution [123], yields

$$\begin{aligned} \langle \vec{k} | \vec{e}_\lambda \cdot \vec{r} | \vec{k}' \rangle &= i \vec{e}_\lambda \cdot \vec{\nabla}_{\vec{k}} \delta^3(\vec{k}' - \vec{k}) \quad (\text{A10}) \\ &= -i \vec{e}_\lambda \cdot \vec{\nabla}_{\vec{k}'} \delta^3(\vec{k}' - \vec{k}). \end{aligned}$$

By letting $\lambda = 0$, i.e., $\vec{e}_0 = \vec{e}_z$, and using the last equality in Eq. (A10), I arrive at Eq. (25).

Appendix B: Saddle-point approximation

The saddle-point approximation or stationary phase approximation [12, 123, 153] is used frequently in strong-field physics to approximate integrals with a highly-oscillating integrand of the form

$$I = \int_{\mathbb{R}^n} f(\vec{x}) e^{-i\mathcal{S}(\vec{x})} d^n x, \quad (\text{B1})$$

with $n \in \mathbb{N}$, $\vec{x} \in \mathbb{R}^n$ and functions $f : \mathbb{R}^n \rightarrow \mathbb{C}$, and $\mathcal{S} : \mathbb{R}^n \rightarrow \mathbb{R}$. The exponential function is assumed to oscillate rapidly and the dominant contribution to I is due to the behavior of the integrand in the vicinity of a single stationary point \vec{x}_0 of $\mathcal{S}(\vec{x})$ which is determined via $\vec{\nabla}_x \mathcal{S}(\vec{x}) = \vec{0}$. The function f shall be continuous and vary comparatively slowly in a compact space around the stationary point \vec{x}_0 which is in its interior. Outside the compact space, f is sufficiently slowly varying such that a negligible contribution is made to I which does not change noticeably, if I let $f(\vec{x}) \approx f(\vec{x}_0)$ there. The following derivation is inspired by the account of Klaiber [154].

I expand \mathcal{S} around \vec{x}_0 in terms of a Taylor series

$$\mathcal{S}(\vec{x}) = \mathcal{S}(\vec{x}_0) + \frac{1}{2!} \sum_{i,j=1}^n \mathcal{H}_S(\vec{x}_0)_{ij} \Delta x_i \Delta x_j + \dots, \quad (\text{B2})$$

where $\vec{x} = \vec{x}_0 + \Delta\vec{x}$ and $\Delta\vec{x} = (\Delta x_1, \dots, \Delta x_n)^T$ [123] and the series needs to converge for $\vec{x} \in \mathbb{R}^n$. There is no first-order term $\frac{1}{1!} \vec{\nabla}_x \mathcal{S}(\vec{x}_0) \cdot \Delta\vec{x}$ in Eq. (B2), as $\vec{\nabla}_x \mathcal{S}(\vec{x}_0) = \vec{0}$. The matrix elements of the Hessian of \mathcal{S} in \vec{x}_0 are $\mathcal{H}_S(\vec{x}_0)_{ij} = \frac{\partial^2 \mathcal{S}(\vec{x}_0)}{\partial x_i \partial x_j}$ for $i, j \in \{1, \dots, n\}$. The Hessian matrix has to be regular, i.e., its determinant $\det \mathcal{H}_S(\vec{x}_0) \neq 0$ and thus its eigenvalues are nonzero. With the expansion (B2), truncated after the second summand, I approximate the integral I [Eq. (B1)] by

$$I \approx I_{\text{st}} = f(\vec{x}_0) e^{-i\mathcal{S}(\vec{x}_0)} \times \int_{\mathbb{R}^n} e^{-\frac{i}{2} \Delta\vec{x}^T \mathcal{H}_S(\vec{x}_0) \Delta\vec{x}} d^n x. \quad (\text{B3})$$

It is sufficient, to assume that f is continuous and slowly varying around \vec{x}_0 . However, if f can be expanded into a Taylor series around \vec{x}_0 which converges in $\vec{x} \in \mathbb{R}^n$, then, in I_{st} , the series expansion of f is understood to be truncated after the zeroth-order term, i.e., $f(\vec{x}) = f(\vec{x}_0) + \dots$. Together with Eq. (B2), this provides a prescription to obtain higher-order corrections to I_{st} in Eq. (B3) and to determine the error of the truncations from the remainder terms of the respective Taylor expansions [123].

The Hessian matrix $\mathcal{H}_S(\vec{x}_0)$ in Eq. (B3) is real-symmetric and thus diagonalizable with an orthogonal matrix $\mathcal{O}(\vec{x}_0)$ where $\mathcal{O}(\vec{x}_0)^{-1} = \mathcal{O}(\vec{x}_0)^T$ [123]. This provides the decomposition $\mathcal{H}(\vec{x}_0) = \mathcal{O}(\vec{x}_0) \mathcal{E}(\vec{x}_0) \mathcal{O}(\vec{x}_0)^T$ where $\mathcal{E}(\vec{x}_0)$ is the diagonal matrix of the real eigenvalues of $\mathcal{H}(\vec{x}_0)$. To simplify the remaining integral in

Eq. (B3), I transform to new coordinates \vec{y} with the diffeomorphism $\Phi_{\vec{x}_0} : \mathbb{R}^n \rightarrow \mathbb{R}^n$, $\vec{y} \mapsto \mathcal{O}(\vec{x}_0) \vec{y} + \vec{x}_0 = \vec{x}$, an affine transformation for which $\mathcal{O}(\vec{x}_0) \equiv \mathcal{J}_\Phi(\vec{x}_0)$ is the Jacobian matrix [123]. This yields

$$I_{\text{st}} = f(\vec{x}_0) e^{-i\mathcal{S}(\vec{x}_0)} \int_{\mathbb{R}^n} e^{-\frac{i}{2} \vec{y}^T \mathcal{E} \vec{y}} d^n y, \quad (\text{B4})$$

where the absolute value of the Jacobian determinant $\det \mathcal{J}_\Phi(\vec{y}_0)$ is unity as $\mathcal{O}(\vec{x}_0)$ is an orthogonal matrix [123]. The remaining integral is known [123] and found from $\int_{-\infty}^{+\infty} e^{-\frac{i}{2} \epsilon y^2} dy = \sqrt{\frac{-2\pi i}{\epsilon}}$ for $\epsilon \in \mathbb{R}$, $\epsilon \neq 0$. The eigenvalues are multiplied in $\det \mathcal{H}(\vec{x}_0) = \det(\mathcal{O}(\vec{x}_0) \mathcal{E}(\vec{x}_0) \mathcal{O}(\vec{x}_0)^T) = \det \mathcal{O}(\vec{x}_0) \det \mathcal{E}(\vec{x}_0) \det \mathcal{O}(\vec{x}_0)^T = \prod_{i=1}^n \mathcal{E}(\vec{x}_0)_{ii}$ because $\det \mathcal{O}(\vec{x}_0) = \det \mathcal{O}(\vec{x}_0)^T$ and $|\det \mathcal{O}(\vec{x}_0)| = 1$. Then I arrive at the integral I [Eq. (B1)] in saddle-point approximation

$$I_{\text{st}} = \sqrt{(-2\pi i)^n} f(\vec{x}_0) e^{-i\mathcal{S}(\vec{x}_0)} \sqrt{(\det \mathcal{H}(\vec{x}_0))^{-1}}. \quad (\text{B5})$$

I use the saddle-point approximation in Eqs. (46), (96), and (101).

Appendix C: Harmonic photon emission

1. Quantum electrodynamic formulation

The recombination of a continuum electron with a hole in the parent ion leads to the emission of a HH photon. This is fluorescence which cannot be treated with semiclassical light fields; instead, quantum electrodynamics (QED) is required [15, 34, 92, 93, 117, 135, 152]. The energy of a photon in the \vec{q} th mode is $\omega_{\vec{q}}$ with $\vec{q} \in \mathbb{V}$ where \mathbb{V} is the set of allowed modes in the volume V that is used to quantize the electromagnetic field. The photon vacuum state is $|0\rangle$ and the photon number state with one HH photon in mode $\vec{q} \in \mathbb{V}$ is denoted by $|1_{\vec{q}}\rangle$. Then the annihilation $\hat{a}_{\vec{q}}$ and creation $\hat{a}_{\vec{q}}^\dagger$ operators for photons in mode $\vec{q} \in \mathbb{V}$ can be expressed by $\hat{a}_{\vec{q}} = |0\rangle \langle 1_{\vec{q}}|$ and $\hat{a}_{\vec{q}}^\dagger = |1_{\vec{q}}\rangle \langle 0|$, respectively. *Nota bene*, I restrict the description to, at maximum, a single HH photon, i.e., multi-HH-photon states are omitted. This is an excellent approximation as multi-HH-photon emission is highly improbable. The Hamiltonian of the free HH photon field is

$$\hat{H}_{\text{EM}} = \sum_{\vec{q} \in \mathbb{V}} \omega_{\vec{q}} \hat{\mathbb{1}}_{\text{el}}^{N/2} \otimes \hat{a}_{\vec{q}}^\dagger \hat{a}_{\vec{q}} = \sum_{\vec{q} \in \mathbb{V}} \omega_{\vec{q}} \hat{\mathbb{1}}_{\text{el}}^{N/2} \otimes |1_{\vec{q}}\rangle \langle 1_{\vec{q}}|, \quad (\text{C1})$$

where I set the energy of the photon vacuum to zero [117, 152].

The electronic structure after recombination is represented by the no-decay $N/2$ -electron atomic electronic

structure Hamiltonian from Eq. (10) times the projector on the number states with one HH photon which is

$$H_E = \left[\sum_{i=1}^{N/2} \hat{\mathbb{1}}_{\text{el}}^{i-1} \otimes \hat{h}_A \otimes \hat{\mathbb{1}}_{\text{el}}^{N/2-i} \right] \otimes \sum_{\vec{q} \in \mathbb{V}} |1_{\vec{q}}\rangle \langle 1_{\vec{q}}|. \quad (\text{C2})$$

I do not include destruction of the $N/2$ -electron ground state with one HH photon as the amplitude of HH photon emission is desired.

The Hamiltonian for HH fluorescence \hat{H}_H is constructed based on Eq. (39) by replacing in \hat{d}_1 the po-

larization vector \vec{e}_H with the operator for the quantized electric field of the HH light [152] which is represented in electric dipole approximation by

$$\hat{E}_H = -i \sum_{\vec{q} \in \mathbb{V}} \sqrt{\frac{2\pi\omega_{\vec{q}}}{V}} [\vec{e}_H^* \otimes \hat{a}_{\vec{q}}^\dagger - \vec{e}_H \otimes \hat{a}_{\vec{q}}], \quad (\text{C3})$$

with the polarization vector $\vec{e}_H = \vec{e}_z$ and propagation of the HH photons along the x axis. The Hamiltonian \hat{H}_H is expressed in terms of the basis states from Sect. II A [Eq. (5)] via

$$\begin{aligned} \hat{H}_H = & -i a'^*(t) \sum_{\vec{q} \in \mathbb{V}} \sqrt{\frac{2\pi\omega_{\vec{q}}}{V}} \left[\sum_{m \in \mathbb{M}_1} \int_{\mathbb{R}^3} |\Phi_0\rangle \otimes |1_{\vec{q}}\rangle \langle a; m | \vec{e}_H^* \cdot \vec{r} | \vec{k}\rangle \langle \Phi_{\vec{k}}^{(m)} | \otimes \langle 0 | d^3k \right. \\ & \left. + \sum_{m \in \mathbb{M}_2} \int_{\mathbb{R}^3} (|\Phi_0\rangle \otimes |1_{\vec{q}}\rangle \langle a; m | \vec{e}_H^* \cdot \vec{r} | \vec{k}\rangle \langle \Phi_{\vec{k}c}^{(m)} | \otimes \langle 0 | - |\Phi_0\rangle \otimes |1_{\vec{q}}\rangle \langle c; m | \vec{e}_H^* \cdot \vec{r} | \vec{k}\rangle \langle \Phi_{\vec{k}a}^{(m)} | \otimes \langle 0 |) d^3k \right] + \text{h.c.} \end{aligned} \quad (\text{C4})$$

Ground-state depletion is accounted for by the factor $a'^*(t)$ [155].

The QED Hamiltonian for the description of the HHG process reads

$$\hat{H}_{\text{QED}} = \hat{H} \otimes |0\rangle \langle 0| + \hat{H}_{\text{EM}} + \hat{H}_E + \hat{H}_H, \quad (\text{C5})$$

with the total $N/2$ -electron Hamiltonian with semiclassical optical-laser and x-ray fields \hat{H} from Eq. (8) here augmented by the projector on the vacuum photon state $|0\rangle \langle 0|$ of the HH field, and Eqs. (C1), (C4), and (C2).

To determine the amplitude of fluorescence, I make a wave packet ansatz similar to Eq. (17) which, however, explicitly includes the photon number states of the HH field. Similar to Ref. 156, I have

$$|\Psi'', t\rangle = \sum_{\vec{q} \in \mathbb{V}} c_{\vec{q}}'(t) e^{-iE_0 t} |\Phi_0\rangle \otimes |1_{\vec{q}}\rangle + |\Psi', t\rangle \otimes |0\rangle, \quad (\text{C6})$$

where $|\Psi', t\rangle$ is taken from Eq. (17), generalized to arbitrary x-ray pulses [Sect. III A], and extended to encompass the vacuum photon state. The first term on the right-hand side of (C6) is needed to describe recombination, in which a continuum electron fills a vacancy in the valence or the core, returning the atom to its electronic ground state $|\Phi_0\rangle$ where the excess energy is emitted in terms of a HH photon in state $|1_{\vec{q}}\rangle$ with mode $\vec{q} \in \mathbb{V}$.

The wave packet (C6) is inserted into the time-dependent Schrödinger equation (18) with the QED Hamiltonian (C5) and projected onto the state $\langle \Phi_0 | \otimes \langle 0 |$ to obtain the same EOM (19) for ground-state depletion—also true for arbitrary x-ray pulses—as was obtained with the semiclassical Hamiltonian (8).

Projecting for $\vec{k} \in \mathbb{R}^3$ onto $\langle \Phi_{\vec{k}}^{(m_1)} | \otimes \langle 0 |$ with $m_1 \in \mathbb{M}_1$

and onto $\langle \Phi_{\vec{k}c}^{(m_2)} | \otimes \langle 0 |$ and $\langle \Phi_{\vec{k}a}^{(m_2)} | \otimes \langle 0 |$ with $m_2 \in \mathbb{M}_2$, respectively, yields EOMs for recombination with a valence hole and a core hole. These EOMs are similar to those in Eqs. (20) and (23), however, I need to allow for arbitrary x-ray pulses [Sect. III A] and the first term on the right-hand side of (C6) which leads to an extra term on the right-hand side of these EOMs. For valence-hole recombination I need to add $+$ $\sum_{\vec{q} \in \mathbb{V}} \sqrt{\frac{2\pi\omega_{\vec{q}}}{V}} \langle \vec{k} | \vec{e}_H \cdot \vec{r} | a; m \rangle a'(t) c_{\vec{q}}'(t)$ with $m \in \mathbb{M}_a$ and for core-hole recombination $- \sum_{\vec{q} \in \mathbb{V}} \sqrt{\frac{2\pi\omega_{\vec{q}}}{V}} \langle \vec{k} | \vec{e}_H \cdot \vec{r} | c; m_2 \rangle e^{i\omega_{\vec{q}} t + i\varphi_{\vec{q}}(t)} a'(t) c_{\vec{q}}'(t)$ with $m_2 \in \mathbb{M}_2$. The extra summands account for changes in the continuum amplitudes $b_a^{(m)}(\vec{k}, t)$ and $b_c^{(m_2)}(\vec{k}, t)$, respectively, because of recombination with HH emission. Yet as I consider only HH photons with $\vec{q} \in \mathbb{V}$, the two terms do not comprise the entire change in the continuum amplitudes, i.e., due to emission of HH photons into mode $\vec{q} \in (\mathbb{R}^3 \setminus \{\vec{0}\}) \setminus \mathbb{V}$ and suitable polarization [152]. As HHG is inefficient, the contributions of these summands is tiny and can be neglected in excellent approximation.

Projecting onto $\langle \Phi_0 | \otimes \langle 1_{\vec{q}} |$ leads to the EOMs for the amplitude to find a fluorescence photon with mode $\vec{q} \in \mathbb{V}$ [compare with Eq. (19)] reading

$$\frac{d}{dt} c_{\vec{q}}'(t) = -i\omega_{\vec{q}} c_{\vec{q}}'(t) - \sqrt{\frac{2\pi\omega_{\vec{q}}}{V}} \mathcal{D}'(t), \quad (\text{C7})$$

with the appropriately-adapted time-dependent $N/2$ -electron dipole transition matrix element $\mathcal{D}'(t)$ from Eq. (40). Then Eq. (C7) can be integrated directly [123]

yielding

$$c'_{\vec{q}}(t) = -\sqrt{\frac{2\pi\omega_{\vec{q}}}{V}} e^{-i\omega_{\vec{q}}t} \int_{-t}^t e^{i\omega_{\vec{q}}t'} \mathcal{D}'(t') dt'. \quad (\text{C8})$$

For vanishing ground-state depletion, a HH emission rate is derived in Sect. C 2; otherwise only a HPNS [135] can be obtained in Sect. C 3.

2. Harmonic photon emission rate

I assume cw optical-laser and x-ray light and no ground-state depletion, i.e., $a'(t) = 1$ and $\Gamma'_0(t) = 0$ for all t . Then $\mathcal{D}'(t')$ can be replaced by a Fourier series (54). I carry out the time integration in Eq. (C8) using

$$\int_{-t}^t e^{-i\omega t'} dt' = 2t \operatorname{sinc}(\omega t), \quad (\text{C9})$$

with the sinus cardinalis [110] for $z \in \mathbb{C}$ which is defined by

$$\operatorname{sinc} z = \begin{cases} \frac{\sin z}{z} & ; z \neq 0 \\ 1 & ; z = 0. \end{cases} \quad (\text{C10})$$

The amplitude of fluorescence photons follows to

$$c'_{\vec{q}}(t) = -\sqrt{\frac{2\pi\omega_{\vec{q}}}{V}} e^{-i\omega_{\vec{q}}t} (2t) \sum_{j \in \{+, -\}} \sum_{K=-\infty}^{\infty} \quad (\text{C11}) \\ \times [\tilde{\mathcal{D}}_{aj, 2K+1} \operatorname{sinc}((2K+1)\omega_L t - \omega_{\vec{q}}t) \\ + \tilde{\mathcal{D}}_{cj, 2K} \operatorname{sinc}(2K\omega_L t + \omega_X t - \omega_{\vec{q}}t)].$$

The probability to find a HH photon at time t in mode $\vec{q} \in \mathbb{V}$ is given by $|c'_{\vec{q}}(t)|^2$. From this, the rate of HH emission into mode \vec{q} follows to $\Gamma_{\vec{q}} = \lim_{t \rightarrow \infty} \frac{|c'_{\vec{q}}(t)|^2}{2t}$. I transform the relation for $\Gamma_{\vec{q}}$, after inserting Eq. (C11), with the representation

$$\lim_{t \rightarrow \infty} (t \operatorname{sinc}^2(\omega t)) = \pi \delta(\omega), \quad (\text{C12})$$

of the Dirac δ distribution [118]. The cross terms in $\Gamma_{\vec{q}}$ for harmonics with different arguments in the sinus cardinalis functions vanish [110] due to

$$\lim_{t \rightarrow \infty} (t \operatorname{sinc}(\omega t) \operatorname{sinc}((\omega + \omega')t)) = 0 \quad (\text{C13})$$

for $\omega' \neq 0$ [157].

The total rate of HH photon emission is $\sum_{\vec{q} \in \mathbb{V}} \Gamma_{\vec{q}}$. As free-photon states are spaced densely, the sum over $\vec{q} \in \mathbb{V}$ can be replaced by an integral $\int_0^\infty d\omega$ over V times the density of free-photon states $\rho(\omega)$ [Eq. (59)]. No angular integration is performed as the propagation direction of the HH photons is fixed along the x axis. Then the integrand represents the angular-resolved (for the chosen angles) spectral rate of HH photon emission where the extra factor of 2 in Eq. (58) accounts for the two possible spin states of electrons per spatial orbital.

3. Harmonic photon number spectrum

The situation of HH emission changes as soon as ground-state depletion is considered by letting $\Gamma'_0(t) > 0$ leading to a decreasing ground-state amplitude $a'^*(t)$ with time $0 \leq t \leq T_P$ in Eq. (C4) for optical-laser and x-ray pulses restricted to this range. In this case, HH emission is not periodic anymore; instead of a HH emission rate, I, therefore, calculate the HPNS [135], i.e., the probability to emit a HH photon into mode $\vec{q} \in \mathbb{V}$ via

$$\lim_{t \rightarrow \infty} |c_{\vec{q}}(t)|^2 = \frac{2\pi\omega_{\vec{q}}}{V} |\tilde{\mathcal{D}}'(\omega_{\vec{q}})|^2, \quad (\text{C14})$$

where the time integral in Eq. (C8) over $\mathcal{D}'(t')$ becomes the Fourier transform $\tilde{\mathcal{D}}'(\omega_{\vec{q}})$ in the limit $t \rightarrow \infty$. The HPNS for a single atom follows by replacing the sum over modes \vec{q} by an integral over $V \rho(\omega)$ [Eq. (59)] yielding Eq. (69) where the extra factor of 2 stems from the two spin states.

-
- [1] A. McPherson, G. Gibson, H. Jara, U. Johann, T. S. Luk, I. A. McIntyre, K. Boyer, and C. K. Rhodes, “Studies of multiphoton production of vacuum-ultraviolet radiation in the rare gases,” *J. Opt. Soc. Am. B* **4**, 595–601 (1987).
 [2] M. Ferray, A. L’Huillier, X. F. Li, L. A. Lompre, G. Mainfray, and C. Manus, “Multiple-harmonic conversion of 1064 nm radiation in rare gases,” *J. Phys. B* **21**, L31–L35 (1988).

- [3] Pierre Agostini and Louis F. DiMauro, “The physics of attosecond light pulses,” *Rep. Prog. Phys.* **67**, 813–855 (2004).
 [4] A. Scrinzi, M. Yu Ivanov, R. Kienberger, and D. M. Villeneuve, “Attosecond physics,” *J. Phys. B* **39**, R1–R37 (2006).
 [5] Philip H. Bucksbaum, “The future of attosecond spectroscopy,” *Science* **317**, 766–769 (2007).
 [6] Ferenc Krausz and Misha Ivanov, “Attosecond physics,” *Rev. Mod. Phys.* **81**, 163–234 (2009).

- [7] Markus C. Kohler, Thomas Pfeifer, Karen Z. Hatsagortsyan, and Christoph H. Keitel, “Frontiers of atomic high-harmonic generation,” *Adv. At. Mol. Opt. Phys.* **61**, 159–208 (2012), arXiv:1201.5094.
- [8] M. Yu. Kuchiev, “Atomic antenna,” *Pis'ma Zh. Eksp. Teor. Fiz.* **45**, 319–332 (1987), *JETP Lett.* **45**, 404–406 (1987).
- [9] Jeffrey L. Krause, Kenneth J. Schafer, and Kenneth C. Kulander, “High-order harmonic generation from atoms and ions in the high intensity regime,” *Phys. Rev. Lett.* **68**, 3535–3538 (1992).
- [10] K. J. Schafer, Baorui Yang, L. F. DiMauro, and K. C. Kulander, “Above threshold ionization beyond the high harmonic cutoff,” *Phys. Rev. Lett.* **70**, 1599–1602 (1993).
- [11] Paul B. Corkum, “Plasma perspective on strong-field multiphoton ionization,” *Phys. Rev. Lett.* **71**, 1994–1997 (1993).
- [12] M. Lewenstein, Ph. Balcou, M. Yu. Ivanov, Anne L’Huillier, and Paul B. Corkum, “Theory of high-harmonic generation by low-frequency laser fields,” *Phys. Rev. A* **49**, 2117–2132 (1994).
- [13] W. Becker, S. Long, and J. K. McIver, “Modeling harmonic generation by a zero-range potential,” *Phys. Rev. A* **50**, 1540–1560 (1994).
- [14] M. Yu. Kuchiev and V. N. Ostrovsky, “Quantum theory of high harmonic generation as a three-step process,” *Phys. Rev. A* **60**, 3111–3124 (1999).
- [15] Dejan B. Milošević, “A semi-classical model for high-harmonic generation,” in *Super-Intense Laser-Atom Physics*, NATO Science Series II: Mathematics, Physics and Chemistry, Vol. 12, edited by Bernard Piraux and Kazimierz Rzażewski (Kluwer Academic Publishers, Dordrecht, Boston, London, 2001) pp. 229–238.
- [16] W. Becker, F. Grasbon, R. Kopold, D. B. Milošević, G. G. Paulus, and H. Walther, “Above-threshold ionization: From classical features to quantum effects,” *Adv. At. Mol. Opt. Phys.* **48**, 35–98 (2002).
- [17] Kenneth J. Schafer, “Numerical methods in strong field physics,” in *Strong Field Laser Physics*, Springer Series in Optical Sciences, Vol. 134, edited by Thomas Brabec (Springer, New York, 2009) pp. 111–145.
- [18] A. L’Huillier, K. J. Schafer, and K. C. Kulander, “Theoretical aspects of intense field harmonic generation,” *J. Phys. B* **24**, 3315–3341 (1991).
- [19] Philippe Balcou, Anne S. Dederichs, Mette B. Gaarde, and Anne L’Huillier, “Quantum-path analysis and phase matching of high-order harmonic generation and high-order frequency mixing processes in strong laser fields,” *J. Phys. B* **32**, 2973–2989 (1999).
- [20] E. Priori, G. Cerullo, M. Nisoli, S. Stagira, S. De Silvestri, P. Villoresi, L. Poletto, P. Ceccherini, C. Altucci, R. Bruzzese, and C. de Lisio, “Nonadiabatic three-dimensional model of high-order harmonic generation in the few-optical-cycle regime,” *Phys. Rev. A* **61**, 063801 (2000).
- [21] Mette B. Gaarde, Jennifer L. Tate, and Kenneth J. Schafer, “Macroscopic aspects of attosecond pulse generation,” *J. Phys. B* **41**, 132001 (2008).
- [22] Tenio Popmintchev, Ming-Chang Chen, Dimitar Popmintchev, Paul Arpin, Susannah Brown, Skirmantas Ališauskas, Giedrius Andriukaitis, Tadas Balčiūnas, Oliver D. Mücke, Audrius Pugzlys, Andrius Baltuška, Bonggu Shim, Samuel E. Schrauth, Alexander Gaeta, Carlos Hernández-García, Luis Plaja, Andreas Becker, Agnieszka Jaron-Becker, Margaret M. Murnane, and Henry C. Kapteyn, “Bright coherent ultrahigh harmonics in the keV x-ray regime from mid-infrared femtosecond lasers,” *Science* **336**, 1287–1291 (2012).
- [23] Marko Swoboda, Thomas Fordell, Kathrin Klünder, J. Marcus Dahlström, Miguel Miranda, Christian Buth, Kenneth J. Schafer, Johan Mauritsson, Anne L’Huillier, and Mathieu Gisselbrecht, “Phase measurement of resonant two-photon ionization in helium,” *Phys. Rev. Lett.* **104**, 103003 (2010), arXiv:1002.2550.
- [24] J. Itatani, J. Levesque, D. Zeidler, Hiromichi Niikura, H. Pépin, J. C. Kieffer, P. B. Corkum, and D. M. Villeneuve, “Tomographic imaging of molecular orbitals,” *Nature* **432**, 867–871 (2004).
- [25] Robin Santra, “Imaging molecular orbitals using photoionization,” *Chem. Phys.* **329**, 357–364 (2006).
- [26] Toru Morishita, Anh-Thu Le, Zhangjin Chen, and C. D. Lin, “Accurate retrieval of structural information from laser-induced photoelectron and high-order harmonic spectra by few-cycle laser pulses,” *Phys. Rev. Lett.* **100**, 013903 (2008).
- [27] C. D. Lin and Junliang Xu, “Imaging ultrafast dynamics of molecules with laser-induced electron diffraction,” *Phys. Chem. Chem. Phys.* **14**, 13133–13145 (2012).
- [28] Robin Santra and Ariel Gordon, “Three-step model for high-harmonic generation in many-electron systems,” *Phys. Rev. Lett.* **96**, 073906 (2006).
- [29] Serguei Patchkovskii, Zengxiu Zhao, Thomas Brabec, and David M. Villeneuve, “High harmonic generation and molecular orbital tomography in multielectron systems,” *J. Chem. Phys.* **126**, 114306 (2007).
- [30] M. F. Kling, Ch. Siedschlag, A. J. Verhoef, J. I. Khan, M. Schultze, Th. Uphues, Y. Ni, M. Uiberacker, M. Drescher, F. Krausz, and M. J. J. Vrakking, “Control of electron localization in molecular dissociation,” *Science* **312**, 246–248 (2006).
- [31] A. L. Cavalieri, N. Müller, Th. Uphues, V. S. Yakovlev, A. Baltuška, B. Horvath, L. Schmidt, B. Blümel, S. Holzwarth, R. Hendel, M. Drescher, U. Kleineberg, P. M. Echenique, R. Kienberger, F. Krausz, and U. Heinzmann, “Attosecond spectroscopy in condensed matter,” *Nature* **449**, 1029–1032 (2007).
- [32] K. C. Kulander and T. N. Rescigno, “Effective potentials for time-dependent calculations of multiphoton processes in atoms,” *Comput. Phys. Commun.* **63**, 523–528 (1991).
- [33] K. C. Kulander, K. J. Schafer, and J. L. Krause, “Dynamics of short-pulse excitation, ionization and harmonic conversion,” in *Super-Intense Laser-Atom Physics*, NATO Advanced Study Institute Series B: Physics, Vol. 316, edited by Bernard Piraux, Anne L’Huillier, and Kazimierz Rzażewski (Plenum Press, New York, 1993) pp. 95–110.
- [34] A. Pukhov, S. Gordienko, and T. Baeva, “Temporal structure of attosecond pulses from intense laser-atom interactions,” *Phys. Rev. Lett.* **91**, 173002 (2003).
- [35] P. M. Paul, E. S. Toma, P. Breger, G. Mullot, F. Augé, Ph. Balcou, H. G. Muller, and P. Agostini, “Observation of a train of attosecond pulses from high harmonic generation,” *Science* **292**, 1689–1692 (2001).
- [36] E. Goulielmakis, M. Schultze, M. Hofstetter, V. S. Yakovlev, J. Gagnon, M. Uiberacker, A. L. Aquila,

- E. M. Gullikson, D. T. Attwood, R. Kienberger, F. Krausz, and U. Kleineberg, "Single-cycle nonlinear optics," *Science* **320**, 1614–1617 (2008).
- [37] L. E. Chipperfield, J. S. Robinson, J. W. G. Tisch, and J. P. Marangos, "Ideal waveform to generate the maximum possible electron recollision energy for any given oscillation period," *Phys. Rev. Lett.* **102**, 063003 (2009).
- [38] J. B. Watson, A. Sanpera, X. Chen, and K. Burnett, "Harmonic generation from a coherent superposition of states," *Phys. Rev. A* **53**, R1962–R1965 (1996).
- [39] A. Sanpera, J. B. Watson, M. Lewenstein, and K. Burnett, "Harmonic-generation control," *Phys. Rev. A* **54**, 4320–4326 (1996).
- [40] Dejan B. Milošević, "Theoretical analysis of high-order harmonic generation from a coherent superposition of states," *J. Opt. Soc. Am. B* **23**, 308–317 (2006).
- [41] D. B. Milošević, "High-energy stimulated emission from plasma ablation pumped by resonant high-order harmonic generation," *J. Phys. B* **40**, 3367–3376 (2007).
- [42] V. Strelkov, "Role of autoionizing state in resonant high-order harmonic generation and attosecond pulse production," *Phys. Rev. Lett.* **104**, 123901 (2010).
- [43] D. B. Milošević, "Resonant high-order harmonic generation from plasma ablation: Laser intensity dependence of the harmonic intensity and phase," *Phys. Rev. A* **81**, 023802 (2010).
- [44] Brian K. McFarland, Joseph P. Farrell, Philip H. Bucksbaum, and Markus Gühr, "High harmonic generation from multiple orbitals in N_2 ," *Science* **322**, 1232–1235 (2008).
- [45] Olga Smirnova, Yann Mairesse, Serguei Patchkovskii, Nirit Dudovich, David Villeneuve, Paul Corkum, and Misha Yu. Ivanov, "High harmonic interferometry of multi-electron dynamics in molecules," *Nature* **460**, 972–977 (2009).
- [46] C. Figueira de Morisson Faria and B. B. Augstein, "Molecular high-order harmonic generation with more than one active orbital: Quantum interference effects," *Phys. Rev. A* **81**, 043409 (2010).
- [47] P. M. Kraus, S. B. Zhang, A. Gijsbertsen, R. R. Lucchese, N. Rohringer, and H. J. Wörner, "High-harmonic probing of electronic coherence in dynamically aligned molecules," *Phys. Rev. Lett.* **111**, 243005 (2013).
- [48] J. Zanghellini, Ch. Jungreuthmayer, and T. Brabec, "Plasmon signatures in high harmonic generation," *J. Phys. B* **39**, 709–728 (2006).
- [49] Ariel Gordon, Franz X. Kärtner, Nina Rohringer, and Robin Santra, "Role of many-electron dynamics in high harmonic generation," *Phys. Rev. Lett.* **96**, 223902 (2006).
- [50] P. Koval, F. Wilken, D. Bauer, and C. H. Keitel, "Non-sequential double recombination in intense laser fields," *Phys. Rev. Lett.* **98**, 043904 (2007).
- [51] Kenichi Ishikawa, "Photoemission and ionization of He^+ under simultaneous irradiation of fundamental laser and high-order harmonic pulses," *Phys. Rev. Lett.* **91**, 043002 (2003).
- [52] Eiji J. Takahashi, Tsuneto Kanai, Kenichi L. Ishikawa, Yasuo Nabekawa, and Katsumi Midorikawa, "Dramatic enhancement of high-order harmonic generation," *Phys. Rev. Lett.* **99**, 053904 (2007).
- [53] Kenichi L. Ishikawa, Eiji J. Takahashi, and Katsumi Midorikawa, "Wavelength dependence of high-order harmonic generation with independently controlled ionization and ponderomotive energy," *Phys. Rev. A* **80**, 011807 (2009).
- [54] S. V. Popruzhenko, D. F. Zaretsky, and W. Becker, "High-order harmonic generation by an intense infrared laser pulse in the presence of a weak UV pulse," *Phys. Rev. A* **81**, 063417 (2010).
- [55] Kenneth J. Schafer, Mette B. Gaarde, Arne Heinrich, Jens Biegert, and Ursula Keller, "Strong field quantum path control using attosecond pulse trains," *Phys. Rev. Lett.* **92**, 023003 (2004).
- [56] Mette B. Gaarde, Kenneth J. Schafer, Arne Heinrich, Jens Biegert, and Ursula Keller, "Large enhancement of macroscopic yield in attosecond pulse train-assisted harmonic generation," *Phys. Rev. A* **72**, 013411 (2005).
- [57] C. Figueira de Morisson Faria, P. Salières, P. Villain, and M. Lewenstein, "Controlling high-order harmonic generation and above-threshold ionization with an attosecond-pulse train," *Phys. Rev. A* **74**, 053416 (2006).
- [58] A. Heinrich, W. Kornelis, M. P. Anscombe, C. P. Hauri, P. Schlup, J. Biegert, and U. Keller, "Enhanced VUV-assisted high harmonic generation," *J. Phys. B* **39**, S275–S281 (2006).
- [59] J. Biegert, A. Heinrich, C. P. Hauri, W. Kornelis, P. Schlup, M. P. Anscombe, M. B. Gaarde, K. J. Schafer, and U. Keller, "Control of high-order harmonic emission using attosecond pulse trains," *J. Mod. Opt.* **53**, 87–96 (2006).
- [60] C. Figueira de Morisson Faria and P. Salières, "High-order harmonic generation with a strong laser field and an attosecond-pulse train: The Dirac-Delta comb and monochromatic limits," *Las. Phys.* **17**, 390–400 (2007).
- [61] Avner Fleischer and Nimrod Moiseyev, "Amplification of high-order harmonics using weak perturbative high-frequency radiation," *Phys. Rev. A* **77**, 010102(R) (2008).
- [62] Avner Fleischer, "Generation of higher-order harmonics upon the addition of high-frequency XUV radiation to IR radiation: Generalization of the three-step model," *Phys. Rev. A* **78**, 053413 (2008).
- [63] Massimo Altarelli, Reinhard Brinkmann, Majed Cherqui, Winfried Decking, Barry Dobson, Stefan Düsterer, Gerhard Grübel, Walter Graeff, Heinz Graafsma, Janos Hajdu, Jonathan Marangos, Joachim Pflüger, Harald Redlin, David Riley, Ian Robinson, Jörg Rossbach, Andreas Schwarz, Kai Tiedtke, Thomas Tschentscher, Ivan Vartanians, Hubertus Wabnitz, Hans Weise, Riko Wichmann, Karl Witte, Andreas Wolf, Michael Wulff, and Mikhail Yurkov, eds., *The Technical Design Report of the European XFEL*, DESY 2006-097 (DESY XFEL Project Group, Deutsches Elektronen-Synchrotron (DESY), Notkestraße 85, 22607 Hamburg, Germany, 2006).
- [64] J. Arthur, P. Anfinrud, P. Audebert, K. Bane, I. Ben-Zvi, V. Bharadwaj, R. Bionta, P. Bolton, M. Borland, P. H. Bucksbaum, R. C. Cauble, J. Clendenin, M. Cornacchia, G. Decker, P. Den Hartog, S. Dierker, D. Dowell, D. Dungan, P. Emma, I. Evans, G. Faigel, R. Falcone, W. M. Fawley, M. Ferrario, A. S. Fisher, R. R. Freeman, J. Frisch, J. Galayda, J.-C. Gauthier, S. Gierman, E. Gluskin, W. Graves, J. Hajdu, J. Hastings, K. Hodgson, Z. Huang, R. Humphry, P. Ilinski, D. Imre, C. Jacobsen, C.-C. Kao, K. R. Kase,

- K.-J. Kim, R. Kirby, J. Kirz, L. Klaisner, P. Krejcik, K. Kulander, O. L. Landen, R. W. Lee, C. Lewis, C. Limborg, E. I. Lindau, A. Lumpkin, G. Materlik, S. Mao, J. Miao, S. Mochrie, E. Moog, S. Milton, G. Mulhollan, K. Nelson, W. R. Nelson, R. Neutze, A. Ng, D. Nguyen, H.-D. Nuhn, D. T. Palmer, J. M. Paterson, C. Pellegrini, S. Reiche, M. Renner, D. Riley, C. V. Robinson, S. H. Rokni, S. J. Rose, J. Rosenzweig, R. Ruland, G. Ruocco, D. Saenz, S. Sasaki, D. Sayre, J. Schmerge, D. Schneider, C. Schroeder, L. Serafini, F. Sette, S. Sinha, D. van der Spoel, B. Stephenson, G. Stupakov, M. Sutton, A. Szöke, R. Tatchyn, A. Toor, E. Trakhtenberg, I. Vasserman, N. Vinokurov, X. J. Wang, D. Waltz, J. S. Wark, E. Weckert, Wilson-Squire Group, H. Winick, M. Woodley, A. Wootton, M. Wulff, M. Xie, R. Yotam, L. Young, and A. Zewail, *Linac Coherent Light Source (LCLS): Conceptual Design Report*, Tech. Rep. SLAC-R-593, UC-414 (Stanford Linear Accelerator Center (SLAC), Menlo Park, California, USA, 2002).
- [65] P. Emma, R. Akre, J. Arthur, R. Bionta, C. Bostedt, J. Bozek, A. Brachmann, P. Bucksbaum, R. Coffee, F.-J. Decker, Y. Ding, D. Dowell, S. Edstrom, J. Fisher, A. Frisch, S. Gilevich, J. Hastings, G. Hays, Ph. Hering, Z. Huang, R. Iverson, H. Loos, M. Messerschmidt, A. Miahnahri, S. Moeller, H.-D. Nuhn, G. Pile, D. Ratner, J. Rzepiela, D. Schultz, T. Smith, P. Stefan, H. Tompkins, J. Turner, J. Welch, W. White, J. Wu, G. Yocky, and J. Galayda, “First lasing and operation of an ångstrom-wavelength free-electron laser,” *Nature Photon.* **4**, 641–647 (2010).
- [66] A. M. Kondratenko and E. L. Saldin, “Generation of coherent radiation by a relativistic-electron beam in an undulator,” *Dokl. Akad. Nauk SSSR* **249**, 843 (1979), [*Sov. Phys. Dokl.* **24**, 986–988 (1979)].
- [67] R. Bonifacio, C. Pellegrini, and L. M. Narducci, “Collective instabilities and high-gain regime in a free electron laser,” *Opt. Commun.* **50**, 373–378 (1984).
- [68] Evgeny L. Saldin, E. A. Schneidmiller, and Mikhail V. Yurkov, *The physics of free electron lasers* (Springer, Berlin, Heidelberg, New York, 2000).
- [69] Thomas Pfeifer, Yuhai Jiang, Stefan Düsterer, Robert Moshhammer, and Joachim Ullrich, “Partial-coherence method to model experimental FEL pulse statistics,” *Opt. Lett.* **35**, 3441–3443 (2010).
- [70] Y. H. Jiang, T. Pfeifer, A. Rudenko, O. Herrwerth, L. Foucar, M. Kurka, K. U. Kühnel, M. Lezius, M. F. Kling, X. Liu, K. Ueda, S. Düsterer, R. Treusch, C. D. Schröter, R. Moshhammer, and J. Ullrich, “Temporal coherence effects in multiple ionization of N₂ via XUV pump-probe autocorrelation,” *Phys. Rev. A* **82**, 041403(R) (2010).
- [71] Stefano M. Cavaletto, Christian Buth, Zoltán Harman, Elliot P. Kanter, Stephen H. Southworth, Linda Young, and Christoph H. Keitel, “Resonance fluorescence in ultrafast and intense x-ray free electron laser pulses,” *Phys. Rev. A* **86**, 033402 (2012), arXiv:1205.4918.
- [72] F. J. Wuilleumier and M. Meyer, “Pump-probe experiments in atoms involving laser and synchrotron radiation: an overview,” *J. Phys. B* **39**, R425–R477 (2006).
- [73] Robin Santra, Christian Buth, Emily R. Peterson, Robert W. Dunford, Elliot P. Kanter, Bertold Krässig, Stephen H. Southworth, and Linda Young, “Strong-field control of x-ray absorption,” *J. Phys.: Conf. Ser.* **88**, 012052 (2007), arXiv:0712.2556.
- [74] Robin Santra, Robert W. Dunford, Elliot P. Kanter, Bertold Krässig, Stephen H. Southworth, and Linda Young, “Strong-field control of x-ray processes,” in *Advances in Atomic, Molecular, and Optical Physics*, Vol. 56, edited by Ennio Arimondo, Paul R. Berman, and Chun C. Lin (Academic Press, Amsterdam, 2008) pp. 219–259.
- [75] Bernhard W. Adams, Christian Buth, Stefano M. Cavaletto, Jörg Evers, Zoltán Harman, Christoph H. Keitel, Adriana Pálffy, Antonio Picón, Ralf Röhlsberger, Yuri Rostovtsev, and Kenji Tamasaku, “X-ray quantum optics,” *J. Mod. Opt.* **60**, 2–21 (2013).
- [76] T. E. Glover, D. M. Fritz, M. Cammarata, T. K. Allison, Sinisa Coh, J. M. Feldkamp, H. Lemke, D. Zhu, Y. Feng, R. N. Coffee, M. Fuchs, S. Ghimire, J. Chen, S. Shwartz, D. A. Reis, S. E. Harris, and J. B. Hastings, “X-ray and optical wave mixing,” *Nature* **488**, 603–608 (2012).
- [77] Isaac Freund and B. F. Levine, “Optically modulated x-ray diffraction,” *Phys. Rev. Lett.* **25**, 1241–1245 (1970).
- [78] Isaac Freund and B. F. Levine, “Optically modulated x-ray diffraction,” *Phys. Rev. Lett.* **26**, 156–156 (1971).
- [79] P. M. Eisenberger and S. L. McCall, “Mixing of x-ray and optical photons,” *Phys. Rev. A* **3**, 1145–1151 (1971).
- [80] Christian Buth, Markus C. Kohler, Joachim Ullrich, and Christoph H. Keitel, “High-order harmonic generation enhanced by xuv light,” *Opt. Lett.* **36**, 3530–3532 (2011), arXiv:1012.4930.
- [81] Markus C. Kohler, Carsten Müller, Christian Buth, Alexander B. Voitkiv, Karen Z. Hatsagortsyan, Joachim Ullrich, Thomas Pfeifer, and Christoph H. Keitel, “Electron correlation and interference effects in strong-field processes,” in *Multiphoton Processes and Attosecond Physics*, Springer Proceedings in Physics, Vol. 125, edited by Kaoru Yamanouchi and Katsumi Midorikawa (Springer, Berlin, Heidelberg, 2012) pp. 209–217, arXiv:1111.3555.
- [82] Christian Buth, Feng He, Joachim Ullrich, Christoph H. Keitel, and Karen Zaveni Hatsagortsyan, “Attosecond pulses at kiloelectronvolt photon energies from high-order harmonic generation with core electrons,” *Phys. Rev. A* **88**, 033848 (2013), arXiv:1203.4127.
- [83] Dejan B. Milošević and A. F. Starace, “Control of high-harmonic generation and laser-assisted x-ray-atom scattering with static electric and magnetic fields,” *Las. Phys.* **10**, 278–293 (2000).
- [84] Dejan B. Milošević and Fritz Ehlötzky, “Scattering and reaction processes in powerful laser fields,” *Adv. At. Mol. Opt. Phys.* **49**, 373–532 (2003).
- [85] Christian Buth, “High-order harmonic generation with resonant core excitation by ultraintense x rays,” (2013), arXiv:1303.1332.
- [86] V. A. Antonov, Y. V. Radeonychev, and Olga Kocharovskaya, “Formation of a single attosecond pulse via interaction of resonant radiation with a strongly perturbed atomic transition,” *Phys. Rev. Lett.* **110**, 213903 (2013).
- [87] M. Tudorovskaya and M. Lein, “High-harmonic generation with combined infrared and extreme ultraviolet fields,” *J. Mod. Opt.* **61**, 845–850 (2014).

- [88] I. I. Rabi, “On the process of space quantization,” *Phys. Rev.* **49**, 324–328 (1936).
- [89] I. I. Rabi, “Space quantization in a gyrating magnetic field,” *Phys. Rev.* **51**, 652–654 (1937).
- [90] I. I. Rabi, J. R. Zacharias, S. Millman, and P. Kusch, “A new method of measuring nuclear magnetic moment,” *Phys. Rev.* **53**, 318–318 (1938).
- [91] Claude Cohen-Tannoudji, Bernard Diu, and Franck Laloë, *Quantum Mechanics* (John Wiley & Sons, New York, 1977).
- [92] Marlan O. Scully and M. Suhail Zubairy, *Quantum Optics* (Cambridge University Press, Cambridge, New York, Melbourne, 1997).
- [93] Pierre Meystre and Murray Sargent III, *Elements of Quantum Optics*, 3rd ed. (Springer, Berlin, 1999).
- [94] Jens Als-Nielsen and Des McMorrow, *Elements of Modern X-Ray Physics* (John Wiley & Sons, New York, 2001).
- [95] J. L. Campbell and Tibor Papp, “Widths of the atomic K–N7 levels,” *At. Data Nucl. Data Tables* **77**, 1–56 (2001).
- [96] A. M. Perelomov, V. S. Popov, and V. M. Terentév, “Ionization of atoms in an alternating electrical field,” *Zh. Exp. Theor. Fiz.* **50**, 1393–1409 (1966), [*Sov. Phys. JETP* **23**, 924–934 (1966)].
- [97] A. M. Perelomov, V. S. Popov, and V. M. Terentév, “Ionization of atoms in an alternating electrical field. II,” *Zh. Exp. Theor. Fiz.* **51**, 309–326 (1966), [*Sov. Phys. JETP* **24**, 207–217 (1967)].
- [98] A. M. Perelomov and V. S. Popov, “Ionization of atoms in an alternating electrical field. III,” *Zh. Exp. Theor. Fiz.* **52**, 514–526 (1967), [*Sov. Phys. JETP* **25**, 336–343 (1967)].
- [99] V. S. Popov, V. P. Kuznetsov, and A. M. Perelomov, “Quasiclassical approximation for nonstationary problems,” *Zh. Exp. Theor. Fiz.* **53**, 331–347 (1967), [*Sov. Phys. JETP* **26**, 222–232 (1968)].
- [100] M. V. Ammosov, N. B. Delone, and V. P. Krainov, “Tunnel ionization of complex atoms and of atomic ions in an alternating electromagnetic field,” *Zh. Eksp. Teor. Fiz.* **91**, 2008–2013 (1986), [*Sov. Phys. JETP* **64**, 1191–1194 (1986)].
- [101] Nikolai B. Delone and Vladimir P. Krainov, *Multiphoton Processes in Atoms*, 2nd ed., edited by P. Lambropoulos, *Atoms and Plasmas*, Vol. 13 (Springer, Berlin, 2000).
- [102] Gennady L. Yudin and Misha Yu. Ivanov, “Nonadiabatic tunnel ionization: Looking inside a laser cycle,” *Phys. Rev. A* **64**, 013409 (2001).
- [103] Nina Rohringer and Robin Santra, “Resonant Auger effect at high x-ray intensity,” *Phys. Rev. A* **77**, 053404 (2008).
- [104] Nina Rohringer and Robin Santra, “Publisher’s Note: Resonant Auger effect at high x-ray intensity [*Phys. Rev. A* **77**, 053404 (2008)],” *Phys. Rev. A* **77**, 059903(E) (2008).
- [105] Nina Rohringer and Robin Santra, “Strongly driven resonant Auger effect treated by an open-quantum-system approach,” *Phys. Rev. A* **86**, 043434 (2012).
- [106] E. P. Kanter, B. Krässig, Y. Li, A. M. March, P. Ho, N. Rohringer, R. Santra, S. H. Southworth, L. F. DiMauro, G. Doumy, C. A. Roedig, N. Berrah, L. Fang, M. Hoener, P. H. Bucksbaum, S. Ghimire, D. A. Reis, J. D. Bozek, C. Bostedt, M. Messerschmidt, and L. Young, “Unveiling and driving hidden resonances with high-fluence, high-intensity x-ray pulses,” *Phys. Rev. Lett.* **107**, 233001 (2011).
- [107] Tenio Popmintchev, Ming-Chang Chen, Alon Bahabad, Michael Gerrity, Pavel Sidorenko, Oren Cohen, Ivan P. Christov, Margaret M. Murnane, and Henry C. Kapteyn, “Phase matching of high harmonic generation in the soft and hard x-ray regions of the spectrum,” *Proc. Natl. Acad. Sci. U.S.A.* **106**, 10516–10521 (2009).
- [108] P. Arpin, T. Popmintchev, N. L. Wagner, A. L. Lytle, O. Cohen, H. C. Kapteyn, and M. M. Murnane, “Enhanced high harmonic generation from multiply ionized argon above 500 eV through laser pulse self-compression,” *Phys. Rev. Lett.* **103**, 143901 (2009).
- [109] M.-C. Chen, P. Arpin, T. Popmintchev, M. Gerrity, B. Zhang, M. Seaberg, D. Popmintchev, M. M. Murnane, and H. C. Kapteyn, “Bright, coherent, ultrafast soft x-ray harmonics spanning the water window from a tabletop light source,” *Phys. Rev. Lett.* **105**, 173901 (2010).
- [110] See the Electronic Supplementary Material for a *Mathematica* [111] Notebook.
- [111] *Mathematica 10.1*, Wolfram Research, Inc., 100 Trade Center Drive, Champaign, Illinois 61820-7237, USA (2015).
- [112] D. R. Hartree, “The wave mechanics of an atom with a non-coulomb central field. Part I. Theory and methods,” *Proc. Camb. Phil. Soc.* **24**, 89–110 (1928).
- [113] Attila Szabo and Neil S. Ostlund, *Modern Quantum Chemistry: Introduction to Advanced Electronic Structure Theory*, 1st, revised ed. (McGraw-Hill, New York, 1989).
- [114] J. C. Slater, “A simplification of the Hartree-Fock method,” *Phys. Rev.* **81**, 385–390 (1951).
- [115] J. C. Slater and K. H. Johnson, “Self-consistent-field $x\alpha$ cluster method for polyatomic molecules and solids,” *Phys. Rev. B* **5**, 844–853 (1972).
- [116] Frank Herman and Sherwood Skillman, *Atomic Structure Calculations* (Prentice-Hall, Englewood Cliffs, New Jersey, 1963).
- [117] Christian Buth and Robin Santra, “Theory of x-ray absorption by laser-dressed atoms,” *Phys. Rev. A* **75**, 033412 (2007), arXiv:physics/0611122.
- [118] Eugen Merzbacher, *Quantum mechanics*, 3rd ed. (John Wiley & Sons, New York, 1998).
- [119] L. Young, D. A. Arms, E. M. Dufresne, R. W. Dunford, D. L. Ederer, C. Höhr, E. P. Kanter, B. Krässig, E. C. Landahl, E. R. Peterson, J. Rudati, R. Santra, and S. H. Southworth, “X-ray microprobe of orbital alignment in strong-field ionized atoms,” *Phys. Rev. Lett.* **97**, 083601 (2006).
- [120] Robin Santra, Robert W. Dunford, and Linda Young, “Spin-orbit effect on strong-field ionization of krypton,” *Phys. Rev. A* **74**, 043403 (2006).
- [121] Nina Rohringer and Robin Santra, “Multi-channel coherence in strong-field ionization,” *Phys. Rev. A* **79**, 053402 (2009).
- [122] Zhi-Heng Loh, Munira Khalil, Raoul E. Correa, Robin Santra, Christian Buth, and Stephen R. Leone, “Quantum state-resolved probing of strong-field-ionized xenon atoms using femtosecond high-order harmonic transient absorption spectroscopy,” *Phys. Rev. Lett.* **98**, 143601 (2007), arXiv:physics/0703149.

- [123] George B. Arfken and Hans J. Weber, *Mathematical Methods for Physicists*, 6th ed. (Elsevier Academic Press, New York, 2005).
- [124] Lorenz S. Cederbaum, W. Domcke, and Jochen Schirmer, “Many-body theory of core holes,” *Phys. Rev. A* **22**, 206–222 (1980).
- [125] G. Angonoa, O. Walter, and Jochen Schirmer, “Theoretical K-shell ionization spectra of N₂ and CO by a fourth-order Green’s function method,” *J. Chem. Phys.* **87**, 6789–6801 (1987).
- [126] Lars Bojer Madsen, “Strong-field approximation in laser-assisted dynamics,” *Am. J. Phys.* **73**, 57–62 (2005).
- [127] Christian Buth and Kenneth J. Schafer, “Theory of Auger decay by laser-dressed atoms,” *Phys. Rev. A* **80**, 033410 (2009), arXiv:0905.3756.
- [128] Robert D. Cowan, *The Theory of Atomic Structure and Spectra*, Los Alamos Series in Basic and Applied Sciences (University of California Press, Berkeley, 1981).
- [129] Los Alamos National Laboratory, Atomic Physics Codes, <http://aphysics2.lanl.gov/tempweb/lanl>.
- [130] Equation (36) is the only expression of this article where the factor $e^{-\eta|t'|}$ is required. Thus I took the limit $\eta \rightarrow 0^+$ in all other equations and, specifically, the factor is omitted from Eq. (12).
- [131] I omit terms for continuum-continuum transitions, i.e., terms involving one-electron matrix elements of the type $\langle \vec{k} | \hat{d}_1 | \vec{k}' \rangle$ for $\vec{k}, \vec{k}' \in \mathbb{R}^3$ [Appendix A 3] because such terms do not play a role for the description of HH emission in the electric dipole transition matrix element in Eq. (39) [12, 14].
- [132] As the electron propagates freely in SFA in the continuum with kinetic momentum \vec{k} , the canonical momentum \vec{p} at time t and at time t' are the same [12].
- [133] I use only the classical part of $S_j^{(m)}(\vec{p}, t, t')$ for the saddle-point approximation, i.e., I let $\mathcal{S}(\vec{p}) = \frac{1}{2} \int_{t'}^t (\vec{p} + \vec{A}_L(t''))^2 dt''$ in Eq. (B1) and include the remaining factors in $f(\vec{p})$. For $S_j^{(m)}(\vec{p}, t, t')$, the series (B2) actually terminates after the second-order term and thus is convergent in the entire \mathbb{R}^3 .
- [134] Morris Edgar Rose, *Elementary Theory of Angular Momentum*, Structure of Matter (John Wiley & Sons, New York, 1957).
- [135] D. J. Diestler, “Harmonic generation: quantum-electrodynamical theory of the harmonic photon-number spectrum,” *Phys. Rev. A* **78**, 033814 (2008).
- [136] The multiplication with the duration T_P corresponds to determining the HPNS from optical-laser and x-ray pulses with constant field strength starting at $t = 0$ and stopping at $t = T_P$ where turn-on effects neglected.
- [137] Jean-Claude Diels and Wolfgang Rudolph, *Ultrashort Laser Pulse Phenomena*, 2nd ed., Optics and Photonics Series (Academic Press, Amsterdam, 2006).
- [138] Ariel Gordon and Franz X. Kärtner, “Quantitative modeling of single atom high harmonic generation,” *Phys. Rev. Lett.* **95**, 223901 (2005).
- [139] Olga Smirnova, Michael Spanner, and Misha Ivanov, “Analytical solutions for strong field-driven atomic and molecular one- and two-electron continua and applications to strong-field problems,” *Phys. Rev. A* **77**, 033407 (2008).
- [140] G. Doumy, C. Roedig, S.-K. Son, C. I. Blaga, A. D. DiChiara, R. Santra, N. Berrah, C. Bostedt, J. D. Bozek, P. H. Bucksbaum, J. P. Cryan, L. Fang, S. Ghimire, J. M. Glowonia, M. Hoener, E. P. Kanter, B. Krässig, M. Kuebel, M. Messerschmidt, G. G. Paulus, D. A. Reis, N. Rohringer, L. Young, P. Agostini, and L. F. DiMauro, “Non-linear atomic response to intense ultrashort x rays,” *Phys. Rev. Lett.* **106**, 083002 (2011).
- [141] Christian Buth, Ji-Cai Liu, Mau Hsiung Chen, James P. Cryan, Li Fang, James M. Glowonia, Matthias Hoener, Ryan N. Coffee, and Nora Berrah, “Ultrafast absorption of intense x rays by nitrogen molecules,” *J. Chem. Phys.* **136**, 214310 (2012), arXiv:1201.1896.
- [142] Kenneth W. DeLong, David N. Fittinghoff, Rick Trebino, Bern Kohler, and Kent Wilson, “Pulse retrieval in frequency-resolved optical gating based on the method of generalized projections,” *Opt. Lett.* **19**, 2152–2154 (1994).
- [143] Rick Trebino, *Frequency-Resolved Optical Gating: The Measurement of Ultrashort Laser Pulses* (Kluwer Academic Publishers, Boston, Dordrecht, London, 2000).
- [144] S. Düsterer, P. Radcliffe, C. Bostedt, J. Bozek, A. L. Cavalieri, R. Coffee, J. T. Costello, D. Cubaynes, L. F. DiMauro, Y. Ding, G. Doumy, F. Grüner, W. Helml, W. Schweinberger, R. Kienberger, A. R. Maier, M. Messerschmidt, V. Richardson, C. Roedig, T. Tschentscher, and M. Meyer, “Femtosecond x-ray pulse length characterization at the Linac Coherent Light Source free-electron laser,” *New J. Phys.* **13**, 093024 (2011).
- [145] M. Meyer, P. Radcliffe, T. Tschentscher, J. T. Costello, A. L. Cavalieri, I. Grguras, A. R. Maier, R. Kienberger, J. Bozek, C. Bostedt, S. Schorb, R. Coffee, M. Messerschmidt, C. Roedig, E. Sistrunk, L. F. DiMauro, G. Doumy, K. Ueda, S. Wada, S. Düsterer, A. K. Kazansky, and N. M. Kabachnik, “Angle-resolved electron spectroscopy of laser-assisted Auger decay induced by a few-femtosecond x-ray pulse,” *Phys. Rev. Lett.* **108**, 063007 (2012).
- [146] M. Hentschel, R. Kienberger, Ch. Spielmann, G. A. Reider, N. Milosevic, T. Brabec, P. Corkum, U. Heinzmann, M. Drescher, and F. Krausz, “Attosecond metrology,” *Nature* **414**, 509–513 (2001).
- [147] G. Sansone, E. Benedetti, F. Calegari, C. Vozzi, L. Avaldi, R. Flammini, L. Poletto, P. Villoresi, C. Altucci, R. Velotta, S. Stagira, S. De Silvestri, and M. Nisoli, “Isolated single-cycle attosecond pulses,” *Science* **314**, 443–446 (2006).
- [148] Arman Cingöz, Dylan C. Yost, Thomas K. Allison, Axel Ruehl, Martin E. Fermann, Ingmar Hartl, and Jun Ye, “Direct frequency comb spectroscopy in the extreme ultraviolet,” *Nature* **482**, 68–71 (2012).
- [149] Linda Young, “Precision measurement: A comb in the extreme ultraviolet,” *Nature* **482**, 45–46 (2012).
- [150] Stefano M. Cavaletto, Zoltán Harman, Christian Buth, and Christoph H. Keitel, “X-ray frequency combs from optically controlled resonance fluorescence,” *Phys. Rev. A* **88**, 063402 (2013), arXiv:1302.3141.
- [151] Stefano M. Cavaletto, Zoltán Harman, Christian Ott, Christian Buth, Thomas Pfeifer, and Christoph H. Keitel, “Broadband high-resolution x-ray frequency combs,” *Nature Photon.* **8**, 520–523 (2014),

arXiv:1402.6652.

- [152] D. P. Craig and T. Thirunamachandran, *Molecular Quantum Electrodynamics* (Academic Press, London, 1984).
- [153] Michael Klaiber, *Relativistische Rekollisionen in starken Laserfeldern*, Dissertation, Ruprecht-Karls-Universität Heidelberg, Fakultät für Physik und Astronomie, Heidelberg, Germany (2007), uniform Resource Name (URN): [urn:nbn:de:bsz:16-opus-78423](https://nbn-resolving.org/urn:nbn:de:bsz:16-opus-78423), HeiDOK – Der Heidelberger Dokumentenserver: <http://www.ub.uni-heidelberg.de/archiv/7842>.
- [154] The derivation of Ref. 153 is restricted to a positive definite Hessian in Eq. (B2) as the square root of the Hessian matrix is needed which is not required here [158].
- [155] All coupling terms that involve a HH photon with continuum states, the “continuum-continuum terms” are negligible.
- [156] Klaus Mølmer and Yvan Castin, “Monte Carlo wavefunctions in quantum optics,” *Quantum Semiclass. Opt.* **8**, 49–72 (1996).
- [157] I determine the cases $\omega = 0$ and $\omega + \omega' = 0$ *not* by inserting 0 into the sinus cardinalis (C10)—which would give $\text{sinc } 0 = 1$ —but by taking the limits $\omega \rightarrow 0$ and $\omega + \omega' \rightarrow 0$, respectively, instead after the limit $t \rightarrow \infty$ has been taken.
- [158] Gene H. Golub and Charles F. van Loan, *Matrix Computations*, 3rd ed. (Johns Hopkins University Press, Baltimore, 1996).